

Adversarial Transfer Learning

GARRETT WILSON and DIANE J. COOK, Washington State University, USA

There is a recent large and growing interest in generative adversarial networks (GANs), which offer powerful features for generative modeling, density estimation, and energy function learning. GANs are difficult to train and evaluate but are capable of creating amazingly realistic, though synthetic, image data. Ideas stemming from GANs such as adversarial losses are creating research opportunities for other challenges such as domain adaptation. In this paper, we look at the field of GANs with emphasis on these areas of emerging research. To provide background for adversarial techniques, we survey the field of GANs, looking at the original formulation, training variants, evaluation methods, and extensions. Then we survey recent work on transfer learning, focusing on comparing different adversarial domain adaptation methods. Finally, we take a look forward to identify open research directions for GANs and domain adaptation, including some promising applications such as sensor-based human behavior modeling.

1 INTRODUCTION

In recent years there has been a large and growing interest in generative adversarial networks (GANs). Pitting two well-matched neural networks against each other, playing the roles of a data discriminator and a data generator, the pair is able to refine each player’s abilities in order to perform functions such as synthetic data generation. Goodfellow et al. [45] proposed this technique in 2014. Since that time, hundreds of papers have been published on the topic [50].

GANs have traditionally been applied to synthetic image generation, but recently researchers have been exploring other novel use cases such as domain adaptation. Supervised learning is arguably the most prevalent use of machine learning and has had much success. However, many common supervised learning methods make an assumption that is not always valid: the training data and testing data are drawn from the same distribution. When these distributions differ but are related, *transfer learning* can be used to transfer what is learned on the training distribution to the testing distribution, which often results in improved performance on the testing data in comparison with inaccurately assuming that the training data and testing data were drawn from the same distribution. A popular case of transfer learning is *domain adaptation*, where the feature space and task remain fixed between a source domain and a separate target domain while the marginal probability distributions differ. As with other cases of transfer learning, the goal of domain adaptation is to achieve strong predictive performance on the target data. Recent advances in domain adaptation performance on image datasets have resulted from the use of adversarial losses, a technique inspired by GANs.

The goal of this paper is to investigate and compare current work in the area that highlights the use of GANs for transfer learning. Figure 1 shows the percentage of GAN-related papers that also mention terms related to transfer learning. For comparison, the chart also includes the traditional use of GANs for data generation (such as image generation). Because the most prevalent transfer learning area overlapping GANs is domain adaptation, in this paper we focus on domain adaptation and the GAN-inspired adversarial domain adaptation techniques.

To provide a background for the use of adversarial techniques in transfer learning, we start by providing a game formulaic explanation of GANs with the alternative interpretations, challenges, variants, and extensions that are found in the literature. We follow this with an overview of transfer learning. We next investigate both non-adversarial and the more recent adversarial approaches to

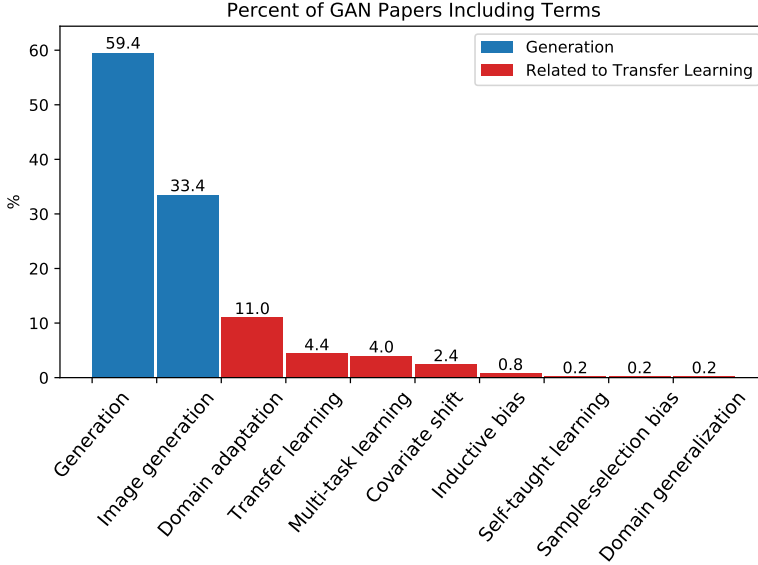


Fig. 1. Of the 500 papers referring to GANs, this figure shows how many of those papers also include terms related to transfer learning (right 8 terms). For comparison, the use of GANs for data generation such as image generation (or synthesis) are included (left 2 terms). Results are based on searching the first three pages of each of the 16,644 available papers published in AAAI, ACL, AISTATS, CVPR, ICLR, ICML, IJCAI, JMLR, and NIPS between January 2014 and August 2018.



Fig. 2. Realistic but entirely synthetic images of human faces generated by a GAN trained on the CelebA-HQ dataset. Images courtesy Karras et al. [62].

domain adaptation. Finally, we identify future research directions for GANs, domain adaptation, and methods of combining and applying these ideas.

To facilitate the comparison of current work in GANs and domain adaptation, we will use image generation and image classification domain adaptation respectively as running examples due to the popularity of these use cases. Popular datasets for GAN-based synthetic image generation include human faces (CelebA [74]), handwritten digits (MNIST [69]), bedrooms (LSUN [125]), and

sets of other objects (CIFAR-10 [66] and ImageNet [26, 107]). A GAN can be trained using such a dataset. Following training, the goal is for the GAN generator to be capable of generating images that closely resemble images in the dataset but that are entirely synthetic. For example, a generator trained with CelebA will generate images of human faces that look realistic but are not images of real people, as shown in Figure 2.

For image classification domain adaptation using GAN-inspired adversarial losses, a model trained on the source image dataset is adapted to perform well on a target image dataset. One use case is unsupervised domain adaptation, where the target dataset is not required to have labels, which can reduce the cost of creating the dataset. For example, we might adapt a model that was trained to recognize traffic signs from computer-generated synthetic instances with known labels [86] to a dataset consisting of photos of real traffic signs [113]. Such adaptation saves the human time that would be spent labeling the images.

2 GENERATIVE ADVERSARIAL NETWORKS

Generative adversarial networks (GANs) are a type of deep generative model [45]. For synthetic image generation, a training dataset of images must be available. After training, the generative model will be able to generate synthetic images that resemble those in the training data. To learn to do this, GANs utilize two neural networks competing against each other [45]. One network represents a generator. The generator accepts a noise vector as input, which contains random values drawn from some distribution such as normal or uniform. The goal of the generator network is to output a vector that is indistinguishable from the real training data. The other network represents a discriminator, which accepts as input either a real sample from the training data or a fake sample from the generator. The goal of the discriminator is to determine the probability that the input sample is real. During training, these two networks play a minimax game, where the generator tries to fool the discriminator and the discriminator tries to not be fooled.

Using the notation from Goodfellow et al. [45], we define a value function $V(G, D)$ employed by the minimax game between the two networks:

$$\min_G \max_D V(D, G) = \mathbb{E}_{x \sim p_{\text{data}}(x)} [\log D(x)] + \mathbb{E}_{z \sim p_z(z)} [\log(1 - D(G(z)))] \quad (1)$$

Here, $x \sim p_{\text{data}}(x)$ draws a sample from the real data distribution, $z \sim p_z(z)$ draws a sample from the input noise, $D(x; \theta_d)$ is the discriminator, and $G(z; \theta_g)$ is the generator. As shown in the equation, the goal is to find the parameters θ_d that maximize the log probability of correctly discriminating between real (x) and fake ($G(z)$) samples while at the same time finding the parameters θ_g that minimize the log probability of $1 - D(G(z))$. The term $D(G(z))$ represents the probability that generated data $G(z)$ is real. If the discriminator correctly classifies a fake input then $D(G(z)) = 0$. Equation 1 minimizes the quantity $1 - D(G(z))$. This occurs when $D(G(z)) = 1$, or when the discriminator misclassifies the generator's output as a real sample. Thus the discriminator's mission is to learn to correctly classify the input as real or fake while the generator tries to fool the discriminator into thinking that its generated output is real. This process is illustrated in Figure 3.

2.1 Components

2.1.1 Generator. Because GANs are generative models, they fit into the generative model taxonomy described by Goodfellow [44] (comparing maximum likelihood variants of the different methods). There are two types of generative models: explicit and implicit. Explicit generative models utilize an explicit density function, therefore the model being learned has an explicit function with parameters that are adjusted to increase the log likelihood of the training data given the parameters. For techniques like fully visible belief nets [10, 36, 41, 68, 94] and change of variables or nonlinear independent components analysis (ICA) models [25, 29], the density function is tractable. For

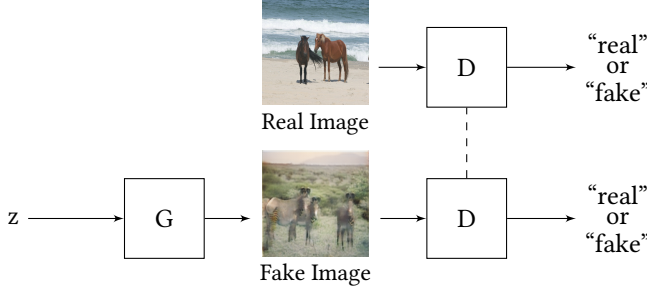


Fig. 3. Illustration of the GAN generator G and discriminator D networks. The dashed line between the D networks indicates that they share weights (or are the same network). In the top row a real image from the training data (horses \leftrightarrow zebras dataset by Zhu et al. [129]) is fed to the discriminator, and the goal of D is to make $D(x) = 1$ (correctly classify as real). In the bottom row a fake image from the generator is fed to the discriminator, and the goal of D is to make $D(G(z)) = 0$ (correctly classify as fake), which competes with the goal of G to make $D(G(z)) = 1$ (misclassify as real).

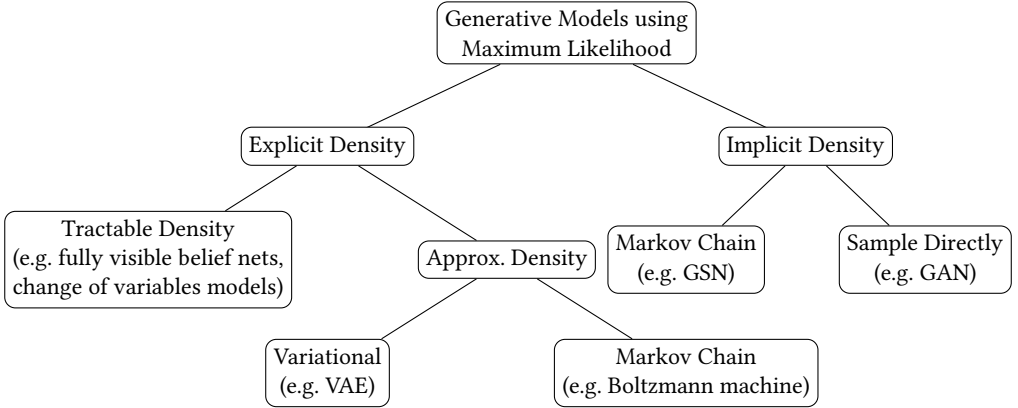


Fig. 4. The generative model taxonomy from Goodfellow [44]. GANs fit into the bottom right leaf. They utilize an implicit density function and sample directly from the distribution in a single step.

variational autoencoders (VAEs) [63, 102] and Boltzmann machines [1, 33, 51], the density function is intractable and thus these methods use approximations. In contrast, implicit generative models do not utilize an explicit density function at all but rather sample from the distribution without modeling it explicitly. Some methods such as generative stochastic networks (GSNs) [11] use a Markov chain to draw samples, but using a Markov chain requires multiple steps and in high dimensional spaces (like images) can be slow to converge [44]. Other methods, like GANs, sample directly from the distribution in one step without the use of a Markov chain [44]. Thus, GANs fit into the generative model taxonomy as having an implicit density function and sampling directly from the distribution in a single step. A summary of the taxonomy is shown in Figure 4.

2.1.2 Discriminator. To learn a generator that can sample directly from the distribution but without relying upon an explicit density function with a tractable log likelihood or an approximation to the log likelihood, GANs use a discriminator, which can be thought of as learning a loss (or cost) function [44, 57]. For this discussion, let's assume that our generator is creating synthetic images

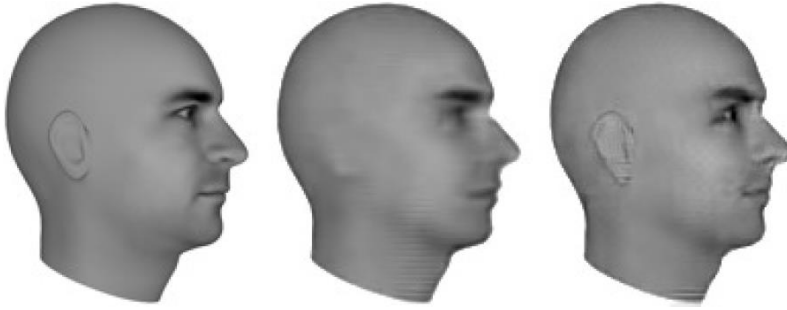


Fig. 5. Ground-truth face (left). Using mean squared error results in the slight alterations of possible human heads being averaged together, blurring the face (middle). An adversarial loss picks one of the possible outputs resulting in a sharper face (right). Images courtesy Lotter et al. [76].

that are close approximations to real images found in a sample dataset. The GAN loss function is $D(x)$, which in Equation 1 represents the discriminator learning to classify input as real or fake. The GAN generator is trained to minimize this loss. Employing alternative loss functions results in subsequent changes to the type of data that is generated. As an example, another loss function is mean-squared error. If this loss function is used, the trained generator would produce blurry images [76] as shown in Figure 5. Intuitively, this outcome is expected because for a given class of images there are multiple realistic outputs that the generator could produce. For example, on a human face there are various slight alterations of hair movement, head rotation, and other features that would look realistic. Mean squared error averages these possibilities and hence generates blurry images [44]. By using a GAN discriminator as a learned loss function, the GAN generator is penalized if it averages together these alterations because it would create images that are easily distinguishable from the real training data.

2.2 Alternative Interpretations

GANs lie at the intersection of many areas of investigation: generative models, deep learning, game theory, probability theory, energy-based models, and reinforcement learning. This has led to a number of alternative interpretations of GANs. These interpretations offer different insights that lead to techniques for improving stability. They could also potentially lead to new and more diverse applications of GANs. Rather than viewing GANs purely as a generative model with a learned loss function, another interpretation is that GANs are learning an energy function which maps to low energy values where the data falls in a high-dimensional space (e.g., where actual CelebA pictures are positioned in the image space) and high energy values everywhere else [127]. GANs offer one way to learn this energy function. The samples from the dataset indicate where the energy function should map to low energy values. In this interpretation, the generator outputs “contrastive samples”, or fake points that the trained energy function maps to high energy values. Markov Chain Monte Carlo methods offer one strategy to generate subsequent samples in a non-parametric way. Alternatively, GANs offer a parametric strategy for generating these contrastive samples – learning the parameters through the GAN minimax game.

GANs can also be interpreted as a way to estimate probabilistic models, i.e., density estimation [90]. In this interpretation, there are two distributions. These are P , the distribution based on the model parameters, and Q , the true data distribution. Given a measure of the distance between P and Q , the GAN essentially adjusts the parameters during training to minimize this distance.

Building on this interpretation, Nowozin et al. [90] generalize GANs for any f -divergence such as Kullback-Leibler, Pearson, or Jensen-Shannon divergence.

Some interpretations of GANs utilize reinforcement learning. Specifically, inverse reinforcement learning (IRL) learns a reward (or cost) function using expert demonstrations of a target task as training data [89]. For example, the demonstrations may be of how bees decide which flowers to visit [89], how humans behave in an economic market [89], how a human drives a car [89], or how to label an image sequence of characters [105]. In the context of GANs, if the generator’s density can be evaluated and is incorporated into the discriminator, Finn et al. [35] showed that GANs are equivalent to maximum entropy IRL. GANs can also be viewed as a type of actor critic approach to reinforcement learning [98]. Both GANs and actor critic methods are multilevel optimization problems in which only the critic (discriminator) has access to the reward (real sample) and the actor (generator) must learn only from the error (gradients) of the critic.

2.3 Training

In recent years there have been impressive results from GANs, fueled in part by the many interpretations that have been considered. At the same time, this research faces a number of challenges. First, training a GAN can encounter problems such as difficulty converging, mode collapse, and vanishing gradients. Second, once successfully trained, the model can be difficult to evaluate and compare with other models. In this section we will look at training challenges followed by a discussion of the evaluation challenges in Section 2.4. There has been much work in both regards, but both problems still require continued research.

2.3.1 Challenges. When training a GAN, multiple challenges may be encountered. GAN training may fail to converge. Because there are two players in the GAN game, each player’s move (i.e., update to its neural network via gradient descent) toward a lower loss may undo the other player’s progress toward reaching its lower loss [44]. For example, GANs have been observed to oscillate without making progress toward an equilibrium [44]. In general, an equilibrium to a game may not even exist (e.g. rock-paper-scissors) [4], but Arora et al. [4] show that an approximate pure equilibrium does exist for a Wasserstein training objective if the generator wins the game. They additionally propose a technique wherein a mixture of discriminators and generators incorporate other objectives. However, while an approximate equilibrium does exist, that does not mean that backpropagation will find it when training the GAN [4].

A common type of non-convergence that GANs may suffer from is *mode collapse*, where the generator only learns to generate realistic samples for a few modes of the data distribution [44]. Oliehoek et al. [93] further classified mode collapse as either *mode omission*, where the generator is unable to generate samples in at least one of the modes of the dataset, or *mode degeneration*, where at least one of the modes is only partially covered. For example, a generator may learn to only generate images of a certain color when the dataset includes images having many colors or of a particular dog when the dataset contains images of many different types of animals [44].

Another problem is *vanishing gradients* illustrated in Figure 6, for which a fix was proposed in the original GAN paper by Goodfellow et al. [45]. A solution to the minimax game is found through iterative optimization: alternating between optimizing the discriminator objective and the generator objective. However, this approach faces a complication since initially when the generated samples are very poor (generated dotted red distribution on the left is far from the true solid blue distribution), the discriminator will be very confident in whether the generated image is real or fake (dashed orange decision boundary on the left easily determines solid blue is real and dotted red is fake). Thus, $D(G(z))$, which is the probability of the generated sample being real, will be very close to zero, making the gradient of $\log(1 - D(G(z)))$ very small (solid blue line is at zero for generated

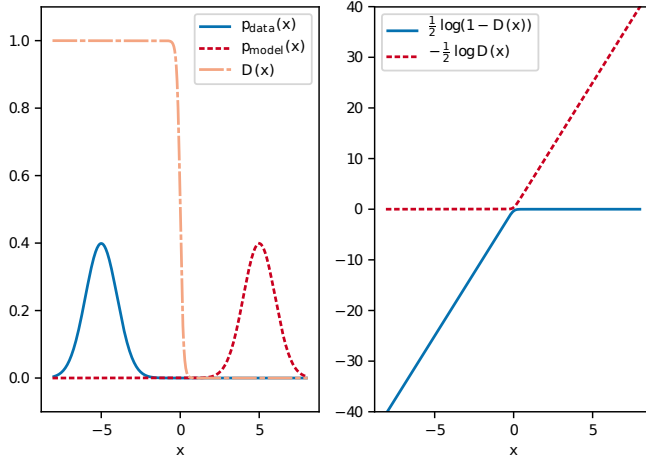


Fig. 6. The true data distribution is shown in solid blue, the currently generated distribution in dotted red, and the discriminator decision boundary in dashed orange (left). The minimax GAN loss is graphed in solid blue and the NS-GAN loss is shown in dotted red (right). Notice that early in training the generator has learned an incorrect distribution shifted to the right of the true distribution. The minimax GAN loss gradient has “vanished” on the right (i.e. is zero) where the generated samples lie ($x \geq 0$) whereas the NS-GAN loss is non-zero and continues to provide a useful gradient. Figure courtesy Fedus et al. [34].

samples on right). This generator optimization problem attempts to minimize the log probability of the discriminator correctly classifying the sample. Alternatively, the optimization objective could be changed to maximize the log probability of the discriminator incorrectly classifying the sample. Thus, Goodfellow et al. [45] suggests replacing the goal of minimizing $\log(1 - D(G(z)))$ with the goal of maximizing $\log(D(G(z)))$ (dotted red line is non-zero for generated samples on right). This is a trick that is commonly used in practice to address vanishing gradients early in training and is referred to as the non-saturating GAN (NS-GAN) [34]. However, Arjovsky et al. [2] later showed that this may remedy vanishing gradients at the cost of decreasing stability.

2.3.2 Tricks. There have been a variety of tricks used to improve the stability of GANs [19], one of which is label smoothing proposed by Salimans et al. [110]. Label smoothing is a technique of replacing the ground-truth probabilities of 1 or 0 with smoothed values such as 0.9 or 0.1. In a GAN discriminator, this decreases the confidence in classifying the input as either real or fake. However, one-sided label smoothing is recommended, wherein only the positive label is smoothed (e.g. to be 0.9) while negative label is kept as 0. If the negative label is smoothed and if the generator’s output is obviously fake, there may not be incentive for it to generate a more realistic output.

These authors also propose applying historical averaging. Using historical averaging, a term is included in each player’s cost to penalize parameters that differ from the historical average of the parameters’ values. In some low-dimensional, continuous non-convex games where gradient descent alone results in orbits and not convergence, this technique has resulted in convergence. Exploring whether historical averaging may help GAN convergence in higher dimensions remains an open question [110].

Along a similar line of thinking but using a history of generated data (such as images) rather than a history of parameter values, Shrivastava et al. [112] propose using a mix of the current

batch of generated images together with past images from a history of generated images when training the discriminator. This both helps training to converge and also makes it less likely for the generator to reintroduce learned artifacts during training since the discriminator is more likely to remember these artifacts are fake.

For a theoretically-backed but trivial to implement improvement, Heusel et al. [49] propose a two time-scale update rule (TTUR): the learning rates of the discriminator and generator differ. These learning rates need to be chosen to balance convergence using a small learning rate and fast training using a large learning rate. Typically the discriminator learning rate will be larger than that of the generator. The authors prove that TTUR results in a GAN converging to a stationary local Nash equilibrium given a few assumptions and empirically demonstrate that it increases training stability and performance.

2.3.3 Network Architectures. In addition to the tricks described in the previous section, commonly some specific network architecture choices are introduced to ease training difficulties. Radford et al. [101] propose DCGAN, five network architecture choices that increase GAN training stability. The first choice is to replace spatial pooling layers with strided convolutions in the discriminator and fractional-strided convolutions in the generator, which require the generator and discriminator to learn how to spatially upsample and downsample, respectively. Second, batch normalization is applied to all layers except for the output layer of the generator and the input layer of the discriminator. Batch normalization is a technique that normalizes the inputs in a batch to have zero mean and unit variance. In their experiments, Radford et al. found this choice helped avoid mode collapse early on, mitigated the effect of poor initialization, and allowed gradients to flow when using very deep networks. Third, fully connected layers can be eliminated. They found that the alternative of using global average pooling improved stability although at the cost of convergence speed. Thus, as a balance between stability and speed, they recommend just eliminating the fully connected layers and relying on the convolutional layers instead. The fourth choice is to use ReLU activations at all generator layers except for the output layer and Tanh for the output layer. Fifth, for the discriminator, leaky ReLU activations can be applied at all layers.

Salimans et al. [110] propose a slight change to batch normalization to help with convergence called *virtual batch normalization*. They found that using just batch normalization resulted in the output of a network for a given input x to be highly dependent on some of the other inputs in a batch. In virtual batch normalization, this problem is remedied by computing statistics on the input x added to a fixed reference data batch chosen at the beginning of training (rather than the current batch).

A drastically different approach was proposed by Karras et al. [62] to progressively grow a GAN for higher and higher image resolution output. Initially they train the generator and discriminator with only a few layers. This generator outputs a small image (e.g. 4x4 pixels). Then they add another layer to the generator and another to the discriminator, which now will output a larger image (e.g. 8x8 pixels). This progressive growth continues till reaching the desired output resolution, which in their case was 1024x1024 pixels. They explain that by introducing this curriculum into the training, rather than learning all small-scale details and large-scale variations in all layers at the same time, during the progressive growth the network has likely already converged at lower-resolution layers and thus only has to learn to refine the smaller representation into a larger representation. As an added benefit, this can accelerate the training process. A potential disadvantage of this approach is that while it generates stunning images (see Figure 2), the method may not work in applications where the individual features are not as related as they are with images.

2.3.4 Objective Modifications. Rather than applying tricks or restricting the network architecture, others have chosen to explore modifying the discriminator or generator objectives in an attempt to

resolve training challenges. Metz et al. [82] introduce unrolled GANs. Their method helps address mode collapse, increase diversity, and stabilize training. When training the generator, they add an auxiliary second term that accounts for how the discriminator will respond to the generator update. They add this auxiliary loss only to the generator since most commonly when training a GAN the discriminator will overpower the generator. By allowing the generator to see one step ahead, the networks will be more balanced. More than one unrolling step could be used, but they found that one was sufficient in their experiments. However, they note for more unstable networks such as recurrent neural networks, likely more than one would be needed.

Arjovsky et al. [3] propose using a Wasserstein GAN (WGAN), and Gulrajani et al. [48] improve upon this with a gradient penalty (WGAN-GP). The original minimax GAN is viewed as minimizing a Jensen-Shannon divergence [45, 90], but this divergence may not always be continuous, which may increase the difficulty of training [3] since training involves computing gradients. Arjovsky et al. show that using the Earth Mover or Wasserstein-1 distance is advantageous because they are continuous everywhere and differentiable almost everywhere, assuming the discriminator is locally Lipschitz. To be k -Lipschitz, the norm of the discriminator's gradients must be upper bounded by k [48], which Arjovsky et al. enforce by clipping the discriminator's weights to be in $[-c, c]$ for some c (e.g. $c = 0.01$). However, Gulrajani et al. found weight clipping on some simple experiments to only learn simple approximations to the optimal model. In addition, the weight clipping can result in vanishing or exploding gradients, requiring careful tuning of c [48]. Instead, they propose replacing the weight clipping with a soft constraint by introducing a gradient penalty term into the discriminator's loss function to penalize norms of gradients far from 1. With this change that results in increased stability, Gulrajani et al. were able to train a variety of architectures and deeper networks, including one that was 101 layers deep. Kodali et al. [64] used a similar gradient penalty in their deep regret analytic GAN (DRAGAN) training method, which helped to avoid mode collapse. However, gradient penalties are not limited to use in WGAN or DRAGAN. Fedus et al. [34] found adding a gradient penalty benefits the original NS-GAN as well.

Jolicœur-Martineau [60] explain that approaches such as WGAN-GP possess a relativistic discriminator: a discriminator that estimates the probability that the real data is *more* realistic than a sample of fake data (or fake data on average), which helps stabilize training. This is in contrast to the original, non-relativistic discriminator that estimates the probability that input data is real (Section 2). Rather than training the generator to make the discriminator output a probability of 1 that the data is real (i.e., fool the discriminator), they suggest both increasing the probability that the fake data is real (toward 0.5) and decreasing the probability that the real data is real (also toward 0.5). This makes use of the *a priori* knowledge that half of a minibatch used during training will be real data and half fake data and better matches the theoretical training dynamics of minimizing the Jensen-Shannon divergence [60]. They show that integral probability metric GANs (IPM-based GANs), which include WGAN and WGAN-GP, are a subset of relativistic GANs (RGANs). They found that using a relativistic discriminator helped to mitigate GANs from becoming stuck early on in training, generated higher-quality samples, allowed for training even on small datasets, and resulted in faster training if including a gradient penalty when compared with WGAN-GP.

Miyato et al. [84] propose a normalization method called *spectral normalization* that stabilizes the discriminator during GAN training. Zhang et al. [126] use spectral normalization for the generator in addition to the discriminator. Spectral normalization GANs (SN-GANs) resulted in higher Inception scores (Section 2.4), increased robustness to changing the network architecture, and was the first to produce reasonable images on the large number of ImageNet classes from a single generator-discriminator pair (i.e., not splitting up the classes among a number of generator-discriminator pairs) [84]. In contrast to weight normalization, SN-GANs generate more diverse and

complex output images but are slightly slower to train. In contrast to WGAN-GP, SN-GANs can handle higher learning rates and are less computationally expensive [84].

Odena et al. [91] introduce Jacobian Clamping. This is a regularization added to the generator loss that attempts to penalize large condition numbers by penalizing singular values of the Jacobian that fall outside a particular range (specified by two hyperparameters). In one of their experiments, they trained a GAN 10 times with different initializations. For half, the condition number initially increased and continued to stay high. Whereas, for the other half, the condition number initially increased and then decreased. They found the condition number to be predictive of GAN performance, as measured by Inception Score and F chet Inception Distance, which are discussed in Section 2.4. By utilizing this regularization to make condition numbers more consistent, they could largely mitigate variance in GAN performance across random network weight initializations.

2.3.5 Combining Methods. These approaches are not all mutually exclusive – a combination of these approaches can aid in training. For example, when Miyato et al. [85] introduce projection-based conditional GANs, they use WGAN-GP for the generator and spectral normalization in the discriminator. Heusel et al. [49] used both their two time-scale update rule along with either DCGAN or WGAN-GP. When Zhang et al. [126] introduce self-attention GANs (SAGANs), they use spectral normalization in both the generator and discriminator and use the two time-scale update rule. They tested this combination and found it allowed training to one million iterations without a decrease in performance (sample quality, FID, and Inception score), whereas with only spectral normalization the performance decreased after around 260,000 iterations [126].

2.3.6 Ongoing Research. There has been much work in regard to resolving training challenges. For a more in-depth discussion of these methods, there are a number of survey papers directed at GAN variants that include a discussion of training challenges and work [52, 54, 79]. However, despite numerous proposed methods to address training challenges, how to ensure GAN training convergence to an equilibrium is an open question that still requires further research.

2.4 Evaluation

Because there are multiple components to a GAN (and multiple uses for a GAN), multiple approaches and measures have been introduced to evaluate GAN performance. Most commonly, the primary GAN model of interest after training is the generator (though some domain adaptation methods discussed in Section 4 end up using part of the discriminator). While training a GAN, the goal of the generator is to fool the discriminator. To do this, it needs to learn to generate samples that are indistinguishable from the training data distribution. Because the distribution may be multi-modal (e.g., images may contain a variety of objects as well as various lighting conditions or locations), the generator must not only learn to generate samples that are indistinguishable from real samples in that mode but also learn to generate samples similarly from every other mode. Not only should a GAN generate realistic samples, but it should ideally also generate diverse samples (avoid mode collapse). Our evaluation should address both of these concerns.

2.4.1 Past Generative Model Evaluation. The de-facto standard for evaluating generative models used for density estimation (the probabilistic interpretations of GANs) is through computing the log-likelihood [117]. The dataset can be split into a training and testing set, and the log-likelihood of the model trained on the training data should achieve high log-likelihood on the testing data (likelihood of the test data should be high given the model) if the generator learned the data distribution well. However, in general computing the log-likelihood in GANs may not be tractable [44]. Recall that in the generative model taxonomy, GANs have an implicit, rather than explicit, density function and they learn the distribution through sampling instead of maximizing log

likelihood or an approximation (see Figure 4). Thus, for evaluation we similarly cannot rely on the log-likelihood and must instead use samples from the generator. At the same time, we need to be careful what methods we use because some sample-based evaluation methods can be misleading [117].

When using log-likelihood is not possible, a Parzen window estimate is commonly used [45, 78, 90, 117]. Using this method, a tractable model is created from generated samples, which then facilitates computing log-likelihood. However, Theis et al. [117] show that this approach should be avoided since in high dimensions the computed log-likelihood may be far from the log-likelihood of the real generator. It may even rank models incorrectly if used for comparison purposes [117].

2.4.2 Realistic Samples. Visually inspecting samples from the generator is common in GANs since most are used for generating images [111]. To evaluate the realism of generated images, Salimans et al. [110] instructed humans (via Amazon Mechanical Turk) to mark which images they thought were generated versus real, from which the researchers could then compare different models.

To provide a more automated evaluation, Salimans et al. [110] propose using an “Inception score” based on the output of running a generated image through an Inception image classification network (see Szegedy et al. [116]). The intuition is that images containing realistic objects will have low entropy in the softmax output layer of the image classification network (low entropy conditional label distribution $p(y|x)$). The low entropy will result from the probability of some objects being high rather than exhibiting a uniform probability distribution over all the possible objects that the classification network can recognize. Furthermore, if the GAN generator outputs images with a large diversity then the marginal distribution $\int p(y|x = G(z))dz$ will have high entropy. This is due to the fact that when integrating over all the possible noise inputs z , the generator outputs a large variety of realistic objects in images rather than only a few select realistic objects. Determining this score requires performing evaluation on a large number of samples [110].

One way for a generator to create exceptionally realistic images (images indistinguishable by a human from the training distribution) is to simply memorize the training data [111], which is an extreme form of overfitting. After training, many researchers thus verify that the generator has not simply memorized the training set. To do this, nearest neighbors in the training data can be computed for the generated images [45] using measures such as Euclidean [78] or cosine [30] distance. If the nearest neighbor is visually almost identical to the training data instance, the generator can be assumed to be memorizing the training data. However, because even a change as simple as shifts of a few pixels can result in the incorrect nearest neighbor based on Euclidean distance (and thus inaccurately concluding that the model is not overfitting), Theis et al. [117] recommends using perceptual distance metrics (e.g. [39, 59, 71]). Instead of pixel-level differences, perceptual distance metrics (or losses) are based on high-level feature differences related to image content [59]. These high-level features are extracted from pre-trained image classification deep CNNs that have already learned hierarchical feature representations [39, 59]. In addition to using perceptual distance metrics, Theis et al. also recommends not limiting the comparison of images to only one nearest neighbor. For example, in the birthday paradox test [5], human evaluators compare 20 closest pairs.

Radford et al. [101] note that if memorization has occurred, then there will be sharp transitions when walking in the learned distribution. Recall that the input to a generator is a noise vector z . This vector represents a space that can be “walked” by changing a single value in the vector while fixing the others and outputting the generated image, then selecting a different value and repeating. If the generator has not memorized the data, then when walking the learned distribution relevant semantic changes should occur. For example, when processing a room image dataset, furniture and other objects might be added or removed. Similarly, when processing a human face image dataset,

the hair style, gender, or expression might change. This approach is similarly used in Berthelot et al. [12].

2.4.3 Diverse Samples. Not only should the generator generate realistic images but it should also generate diverse images, matching the full training distribution. Arora et al. [5] propose the birthday paradox test to determine how well a GAN has generalized to the entire training distribution. The birthday paradox test is inspired by the *birthday paradox*. Imagine there are n people in a room. How large does n need to be in order to have a high probability that 2 people in the room share the same birthday? To guarantee it, $n > 366$ by the pigeonhole principle. However, to have probability $> 50\%$, surprisingly n only needs to be about 23 (assuming birthdays are i.i.d.) [5], which is the “paradox”.

This birthday paradox test uses human evaluation to estimate an upper bound on the support size of the learned generator distribution by checking for duplicates. If a distribution has support n , then likely there will be a duplicate in \sqrt{n} samples drawn from that distribution [5]. Here, “support” refers to the training examples used to specify the learned distribution. This is similar to how “support vectors” in SVMs represent the training examples with non-zero alphas, or the training examples that are used to specify the decision boundary [22, 95]. If only a few training examples are used to learn the generator distribution, then this indicates mode collapse, where the generator no longer can generate diverse images. In the case of generating human face images, such a generator might only generate smiling males with blonde hair. With a small support size, a GAN may only be learning a small portion of the distribution rather than the full distribution.

The birthday paradox test [5] is performed by generating a sample of s images. The 20 closest pairs of that sample can be found using a distance metric such as Euclidean distance (which they found to work on the celebrity face dataset but will likely create issues on other datasets for the previously-noted reasons). Next, a human looks at the 20 images and identifies any near duplicates. This process is repeated multiple times, and if there is high probability that there are near duplicates in each set of 20 images, then likely the support size of the generator distribution is approximately upper bounded by s^2 . If s^2 is too small, then the GAN may be generating realistic outputs, but it suffers from mode collapse and will not be able to generate diverse images throughout the entire training distribution. The one failure mode of this test occurs when the generator creates a few images with high probability (e.g. outputs one image 10 percent of the time), which would result in duplicate images being found in a set of 20 even though the support size may be very large [5].

However, the birthday paradox test still requires human interaction. To minimize human involvement, Santurkar et al. [111] propose a completely automated test of diversity through detecting covariate shift by classification. They train an unconditional GAN and a multi-class classifier on the dataset. Then they create a fake dataset using the GAN generator. They run the multi-class classifier on this fake dataset and compare the results with that on the real dataset. If the GAN learns the true distribution, then there should not be any covariate shift. However, if the GAN suffers from mode collapse, only generating part of the distribution, then there will be a covariate shift. The multi-class classifier can be chosen at varying difficulty or number of classes to determine the extent of the mode collapse.

If using labeled images, Odena et al. [92] propose another entirely automated metric diversity measure by using multi-scale structural similarity (MS-SSIM). MS-SSIM is a human-perception metric yielding higher values for visually similar images. Odena et al. repurpose this for measuring generator diversity by randomly sampling 100 image pairs from each image class. In this case, lower MS-SSIM scores indicate lower perceptual similarity and thus higher diversity. They could detect mode collapse early during training by calculating the mean of these scores on generated images. After training, they could compare the mean scores of the generated images with the real training

data as a measure of the final generator diversity. However, Karras et al. [62] found that MS-SSIM is able to detect large-scale mode collapse but that it misses smaller-scale lack of variation.

2.4.4 Both Realistic and Diverse Samples. An improvement over the Inception score is the F chet Inception Distance (FID) [49]. FID computes a distance between the real and generated distributions, taking advantage of training data statistics (in this case, mean and covariance). This distance will increase both with poorer-quality images and images exhibiting lesser diversity if only a few images are generated for a class [77]. However, it cannot detect memorization of the training set [77]. To compute the score, they use an Inception network and select one layer of the network (with an assumption that the layer’s output is a multidimensional Gaussian). All of the real data samples are input to the network, then mean and variance of the chosen layer’s output are calculated. The next step is to repeat the calculation of mean and variance for 50,000 generated samples. Finally, the F chet distance is computed between these two sets of means and variances [49].

A further improvement is the Class-Aware Fr chet Distance (CAFD). Liu et al. [73] highlight some cases where FID does not correlate well with human judgments but their proposed CAFD evaluation does. Instead of using an Inception network, they train an encoder on the GAN training data to get a domain-specific feature representation. The network used for FID and the Inception score is trained on ImageNet and learns features mostly based on color and shape, which may not work well on other datasets. CAFD assumes a multivariate Gaussian mixture model rather than a multivariate Gaussian, which they propose will avoid losing class information on multi-class datasets. By comparing the results between the training and testing sets, CAFD can provide an indication of the level of overfitting [73].

Yet another automated metric is an approximation of log-likelihood. Wu et al. [123] propose employing annealed importance sampling to calculate log-likelihoods. This could be used for an automated method of detecting memorization as well as offer another human evaluation-based method of checking for diversity. Using a hold-out testing set of images, if the training and testing log-likelihoods throughout training are approximately the same, then the model is considered to be not memorizing the training data [123]. To check for diversity, on both the training and testing set they apply annealed importance sampling to approximate z from their image input x and then generate new outputs based on z . As in the other human evaluation tests, a human can then check for diversity. These authors validated the annealed importance sampling algorithm through bidirectional Monte Carlo. They assume a Gaussian observation model with fixed variance, but they also show that this assumption alone could not account for the detected differences between methods in their validation. Yet, this likely means the approach will also have similar difficulties as the Parzen window estimates in high dimensions [77]. In addition, log-likelihood and visually realistic samples are largely independent. Theis et al. [117] showed that a model could have poor log-likelihood and generate great samples, great log-likelihood and generate poor samples, or good log-likelihood and generate great samples. Grover et al. [46] similarly found a disconnect even in a GAN with tractable log-likelihood. Thus, if the goal is visually realistic samples, log-likelihood (or an approximation of it) is not a satisfactory evaluation metric.

2.4.5 Ongoing Research. Various modifications to the above metrics and some less-commonly-used alternatives have been proposed, which are included in a survey by Borji [14]. Yet, there remains no consensus on how to evaluate GANs. This is a key challenge for continued work on GANs. In fact, when GAN variants were given a large computational budget, Lucic et al. [77] did not find the variants any better than the original NS-GAN by Goodfellow et al. [45] (when evaluated with FID on 4 popular datasets and approximate precision, recall, and F1 on a synthetic convex polygons dataset). In order to develop improvements to GANs, one must have a way of detecting improvement. Thus, GAN evaluation continues to be an ongoing area of research.

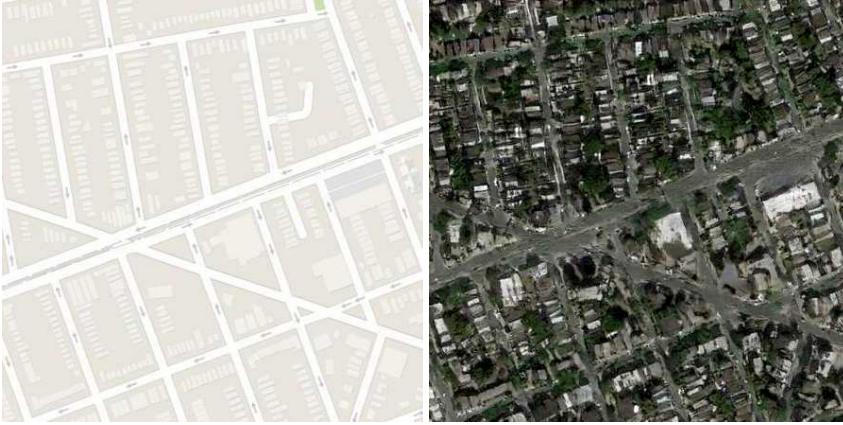


Fig. 7. A satellite view image (right) generated from Google Maps data (left). Images courtesy Isola et al. [57].

2.5 Extensions and Applications

As shown in Sections 2.3 and 2.4, there has been much work on improving GAN training and evaluation. GANs have also been extended for learned inference and conditioning on a class label or input image. There has also been work applying the GAN-inspired idea of an adversarial loss to a variety of problems, in addition to the popular use for generating synthetic images.

2.5.1 Conditional GANs. GANs only accept as input a noise vector (this original formulation is an unconditional GAN). Conditional GANs, on the other hand, accept as input other information such as a class label, image, or other data [28, 40, 45, 83]. In the case of image generation, this means that a particular type of image can be specified to generate. One such example is to generate an image of a particular class within an image dataset such as “cat” rather than a random object from the dataset.

Examples of popular and general-purpose conditional GANs are pix2pix by Isola et al. [57] and CycleGAN by Zhu et al. [129]. These GANs perform image-to-image translation. CycleGAN is based on pix2pix but does not require the training examples to be pairs in the two domains of interest, making CycleGAN entirely unsupervised. CycleGAN accomplishes this by integrating an additional loss function. In addition to the adversarial loss, CycleGAN uses a cycle consistency loss. This means that after translating an image from one domain (e.g. Google Maps data) to another (e.g. Google Maps satellite view), the new image can be translated back to reconstruct the original image. A method that is similar to CycleGAN but is also multimodal is the multimodal unsupervised image-to-image translation (MUNIT) by Huang et al. [56]. By assuming a decomposition into style (domain-specific) and content (domain-invariant) codes, MUNIT can generate diverse outputs for a given input image (e.g. multiple possible satellite view output images).

Some of the many uses of conditional GANs have been: transferring style (e.g. make a photo look like a Van Gogh painting) [129], image colorization [57], generating satellite images from Google Maps data (or vice versa) [57, 129] as shown in Figure 7, converting labels to photos (e.g. semantic segmentation output to a photo) [57, 129], and domain adaptation (e.g. change from a synthetic vehicle driving image to one that looks realistic as shown in Figure 8 and discussed in Sections 4.2.2 and 4.2.3).

2.5.2 Inverse Mapping / Learned Inference. In the original GAN formulation, the generator would accept z as input and output a vector x that is indistinguishable from the training data. In this



Fig. 8. Synthetic vehicle driving image (left) adapted to look realistic (right). Images courtesy Hoffman et al. [53].

formulation there is no way to go from x back to z . Going from the generated data x back to the latent space z is the inverse mapping problem [30], otherwise referred to as learned approximate inference [45]. This problem was explored simultaneously by Donahue et al. [30], who developed bidirectional GANs (BiGAN), and Dumoulin et al. [32], who developed adversarially learned inference (ALI).

2.5.3 Adversarial Loss. Adversarial losses, an idea stemming from GANs, have been applied in multiple settings outside of generative modeling. Wang et al. [121] created an adversarial spatial dropout network to add occlusions to images to improve the accuracy of object detection algorithms. They also created an adversarial spatial transformer network to add deformations such as rotations to objects to again increase object detection accuracy. In other application domains, Pinto et al. [99] used adversarial agents to improve a robot’s ability to grasp an object via self-supervised learning by employing both shaking and snatching adversaries. Giu et al. [47] used an adversarial loss to predict and demonstrate (i.e., robot will copy) human motion. Rippel et al. [103, 104] used a reconstruction and adversarial loss with an autoencoder for learning higher quality image compression at low bit rates. In the next two sections, we will discuss transfer learning and then focus on GAN-inspired adversarial domain adaptation applications, which offer additional use cases for adversarial losses.

3 TRANSFER LEARNING

Transfer learning is defined as the learning scenario where a model is trained on a source domain or task and evaluated on a different but related target domain or task, where either the tasks or domains (or both) differ [31, 96, 122]. For instance, we may wish to learn a model on a handwritten digit dataset (e.g. MNIST [69]) with the goal of using it to recognize house numbers (e.g. SVHN[88]). Or, we may wish to learn a model on a synthetic, cheap-to-generate traffic sign dataset (e.g. [86]) with the goal of using it to classify real traffic signs (e.g. GTSRB [113]). In these examples, the source dataset used to train the model is related but different from the target dataset used to test the model – both are digits and signs respectively but each dataset looks significantly different. When the source and target differ but are related, then transfer learning can be applied to obtain higher accuracy on the target data.

3.1 Terminology

3.1.1 Categorizing Methods. In a transfer learning survey paper, Pan et al. [96] defined two terms to help classify various transfer learning techniques: “domain” and “task.” A domain consists of a feature space and a marginal probability distribution, i.e. the features of the data and the distribution of those features in the dataset. A task consists of a label space and an objective predictive function, i.e. the set of labels and the learned predictive function (learned from the training data). Thus, a transfer learning problem might be either transferring from a source domain to a different target

domain or transferring from a source task to a different target task (or a combination of both) [31, 96, 122].

By this definition, a change in domain may result from either a change in feature space or a change in the marginal probability distribution. When classifying documents using text mining, a change in the feature space may result from a change in language (e.g. English to Spanish) whereas a change in the marginal probability distribution may result from a change in document topics (e.g. computer science to English literature) [96]. Similarly, a change in task may result from either a change in the label space or a change in the objective predictive function. In the case of document classification, a change in the label space may result from a change in the number of classes (e.g. from a set of 10 topic labels to a set of 100 topic labels). Similarly, a change in the objective predictive function may result from a large change in the distribution of the labels (e.g. the source domain has 100 instances of class A and 10,000 of class B, whereas the target has 10,000 instances of A and 100 of B) [96].

To classify transfer learning algorithms based on whether the task or domain differs between source and target, Pan et al. [96] introduced three terms: “inductive”, “transductive”, and “unsupervised” transfer learning. In inductive transfer learning, the target and source tasks are different and the domains may or may not differ, and some labeled target data is required. In transductive transfer learning, the tasks remain the same while the domains are different, and both labeled source data and unlabeled target data are required. Finally, in unsupervised transfer learning, the tasks differ as in the inductive case, but there is no requirement of labeled data in either the source domain or the target domain.

3.1.2 Domain Adaptation. One popular type of transfer learning that has recently been explored as a novel use of GANs is *domain adaptation*, which will be the focus of our transfer learning survey. Domain adaptation is a type of transductive transfer learning. Here, the task remains the same, as does the domain feature space, but the domain marginal probability distributions differ [96, 100]. Only part of the domain changes since the feature space is required to remain fixed between source and target.

In addition to the previous terminology, machine learning techniques are often categorized based on whether or not labeled training data is available. Supervised learning assumes labeled data is available, semi-supervised learning utilizes both labeled data and unlabeled data, and unsupervised learning utilizes only unlabeled data. However, domain adaptation assumes data comes from both a source domain and a target domain. Thus, prepending one of these three terms to “domain adaptation” is ambiguous since it may refer to labeled data being available in the source or target domains.

Authors apply these terms in various ways to domain adaptation [122] (e.g. [23, 58, 96, 109]). In this paper, we will refer to “unsupervised” domain adaptation as the case having labeled source data and unlabeled target data, “semi-supervised” domain adaptation as the case having labeled source data in addition to some labeled target data, and “supervised” domain adaptation as the case having labeled source and target data [8]. This essentially means the adjective is referring to the target domain, which resolves the ambiguity but limits you to domain adaptation where you have source labels. These definitions are commonly used in the methods surveyed in the next section (e.g. used by [37, 44, 75, 109]).

3.1.3 Related Problems. Multi-domain learning [31, 61] and multi-task learning [17] are related to transfer learning and domain adaptation. In contrast to transfer learning, these learning approaches have the goal of obtaining high performance on all specified domains (or tasks) rather than just on a single target domain (or task) [96, 124]. For example, often it is assumed that the training data is drawn in an independent and identically distributed (i.i.d.) fashion, which may not be the

case [61]. One such example is the task of developing a spam filter for users who disagree on what is considered spam. If all the users' data are combined, the training data will consist of multiple domains. While each individual domain may be i.i.d., the aggregated dataset may not be. If the data is split by user, then there may be too little data to learn a model for each user. Multi-domain learning can take advantage of the entire dataset to learn individual user preferences [31, 61]. When working with multiple tasks, instead of training models separately for different tasks (e.g. one model for detecting shapes in an image and one model for detecting text in an image), multi-task learning will learn these separate but related tasks simultaneously so that they can mutually benefit from the training data of other tasks through a (partially) shared representation [17]. If there are both multiple tasks and domains, then these approaches can be combined into multi-domain multi-task learning, as is described by Yang et al. [124].

Another related problem is domain generalization, in which a model is trained on multiple source domains with labeled data and then tested on a separate target domain that was not seen at all during training [87]. This contrasts with domain adaptation where target examples (generally unlabeled) are available during training. Adversarial approaches have been designed to address this situation. Examples include an adversarial method introduced by Zhao et al. [128] and an autoencoder approach by Ghifary et al. [42]:

Zhao et al. [128] propose an adversarial approach for sleep-stage classification from radio frequency (RF) signals. They want to learn a model based on a dataset collected from a number of people in selected environments capable of generalizing well to new people and/or new environments (e.g., sleeping in a different room). This is a domain generalization problem: given multiple source domains the model needs to generalize to an unseen target domain [87]. In the sleep-stage classification setting, the source domains are a person-and-environment pair. Their feature extractor consists of a convolutional neural network (CNN) for extracting stage-specific features from an RF spectrogram and a recurrent neural network (RNN) for extracting time-dependent features. To help the model generalize, their adversarial training method removes conditional dependencies between the source domain and the learned representation through conditioning the discriminator on the predicted label distribution. In other words, the feature extractor is learned such that the discriminator can not determine what source domain the learned representation came from. The result of this approach was a novel and effective strategy for sleep stage classification.

Ghifary et al. [42] propose extending a denoising autoencoder to improve object recognition generalizability. Denoising autoencoders try to reconstruct the original image from a corrupted or noisy version fed into the network. Ghifary et al. instead treat a different view of the data (e.g. rotation, change in size, or variation in lighting) as the corruption or noise. They feed in an input image of an object from one domain and try reconstructing the corresponding views of the object in the other domains. By training in this way, the autoencoder learns features robust to variations across domains. After learning the representation, the feature extractor from the trained autoencoder can be used in a classification task such as object recognition.

3.2 Theory

Now that we have introduced various types of transfer learning, we address the question of needing to know when applying them may be beneficial. Ben-David et al. [9] developed a theory that answers two questions: (1) when will a classifier trained on the source data perform well on the target data, and (2) given a small number of labeled target examples, how can they best be used during training to minimize target test error?

Answering the first question, labeled source data and unlabeled target data are required (unsupervised). Answering the second question, additionally some labeled target data are required (semi-supervised). The answers to both of these questions hold for not only domain changes but

also task changes (e.g. labels can differ). These authors also address the case of multiple source domains, as do Mansour et al. [80]. In this paper, we will focus on the cases containing only one source and one target (as is common in the methods we survey).

3.2.1 When to use transfer learning. With respect to the first question posed in the previous section, a proposed approach is to set a bound on the target error based on the source error and the divergence between the source and target domains [9]. The empirical source error is easy to obtain by first training and then testing a classifier. However, the divergence between the domains cannot be directly obtained with standard methods like Kullback-Leibler divergence due to only having a finite number of samples from the domains and not assuming any particular distribution. Thus, an alternative is to measure using a classifier-induced divergence called $\mathcal{H}\Delta\mathcal{H}$ -divergence. Estimates of this divergence with finite samples converges to the real $\mathcal{H}\Delta\mathcal{H}$ -divergence. This divergence can be estimated by measuring error when getting a classifier to discriminate between the unlabeled source and target examples, though it is often intractable to find the theoretically-required divergence upper bound. Using the source error (right-hand side term 1 of Equation 2), the upper bound on the true $\mathcal{H}\Delta\mathcal{H}$ -divergence (terms 2 and 3) and best hypothesis for the source and target (term 4), the target error can be bounded as shown in Equation 2, with probability at least $1 - \delta$ for $\delta \in (0, 1)$.

$$\epsilon_T(h) \leq \epsilon_S(h) + \frac{1}{2} \hat{d}_{\mathcal{H}\Delta\mathcal{H}}(\mathcal{U}_S, \mathcal{U}_T) + 4\sqrt{\frac{2d \log(2m') + \log(\frac{2}{\delta})}{m'}} + \lambda \quad (2)$$

Here, $\epsilon_T(h)$ is the target error, $\epsilon_S(h)$ is the source error, $\hat{d}_{\mathcal{H}\Delta\mathcal{H}}(\mathcal{U}_S, \mathcal{U}_T)$ is the divergence estimate from the unlabeled source and target examples, d is the VC-dimension, m' is the number of source and target examples (assumed to be the same), and λ is the ideal predictor error.

To summarize, if λ is large, then there is no good hypothesis from training on the source domain that will work well on the target domain. However, as is more common in the application of domain adaptation, if λ is small, then the bound depends on the source error and the $\mathcal{H}\Delta\mathcal{H}$ -divergence [9].

3.2.2 Given some target labels. For the second question, a linear combination of the source and target errors is computed, called the α -error. A bound can be calculated on the true α -error based on the empirical α -error. Finding the minimum α -error depends on the empirical α -error, the divergence between source and target, and the number of labeled source and target examples. Experimentation can be used to empirically determine the values of α that will perform well. These authors demonstrate the process on sentiment classification [9], illustrating that the optimum uses non-trivial values.

The bound is given in Equation 3. If S is a labeled sample of size m with $(1 - \beta)m$ points drawn from the source distribution and βm from the target distribution, then with at least probability $1 - \delta$ for $\delta \in (0, 1)$:

$$\begin{aligned} \epsilon_T(\hat{h}) \leq & \epsilon_T(h_T^*) + 4\sqrt{\frac{\alpha^2}{\beta} + \frac{(1 - \alpha)^2}{1 - \beta}} \sqrt{\frac{2d \log(2(m + 1)) + 2 \log(\frac{8}{\delta})}{m}} + \\ & 2(1 - \alpha) \left(\frac{1}{2} \hat{d}_{\mathcal{H}\Delta\mathcal{H}}(\mathcal{U}_S, \mathcal{U}_T) + 4\sqrt{\frac{2d \log(2m') + \log(\frac{8}{\delta})}{m'}} + \lambda \right) \end{aligned} \quad (3)$$

Here, $\hat{h} \in \mathcal{H}$ is the empirical minimizer of the α -error on S given by $\hat{\epsilon}_\alpha(h) = \alpha \hat{\epsilon}_T(h) + (1 - \alpha) \hat{\epsilon}_S(h)$ and $h_T^* = \min_{h \in \mathcal{H}} \epsilon_T(h)$ is the target error minimizer.

Then, the optimum α is:

$$\alpha^*(m_T, m_S; D) = \begin{cases} 1 & m_T \geq D^2 \\ \min\{1, v\} & m_T \leq D^2 \end{cases} \quad (4)$$

Here, $m_S = (1 - \beta)m$ is the number of source examples, $m_T = \beta m$ is the number of target examples, $D = \sqrt{d}/A$, and

$$v = \frac{m_T}{m_T + m_S} \left(1 + \frac{m_S}{\sqrt{D^2(m_S + m_T) - m_S m_T}} \right) \quad (5)$$

$$A = \frac{1}{2} \hat{d}_{\mathcal{H}\Delta\mathcal{H}}(\mathcal{U}_S, \mathcal{U}_T) + 4\sqrt{\frac{2d \log(2m') + \log(\frac{4}{\delta})}{m'}} + \lambda \quad (6)$$

$$B = 4\sqrt{\frac{2d \log(2(m+1)) + 2 \log(\frac{8}{\delta})}{m}} \quad (7)$$

In summary, when only source or target data is available that data can be used. If the source and target are the same, then $\alpha^* = \beta$, which implies a uniform weighting of examples. Given enough target data, source data should not be used at all because it might increase the test-time error. Furthermore, without enough source data using it may also not be worthwhile, i.e. $\alpha^* \approx 0$ [9].

4 DOMAIN ADAPTATION METHODS

Examining methods for domain adaptation, we will consider non-adversarial domain adaptation. Numerous papers have been written on this topic including other survey papers [8, 81, 97] so we focus primarily on neural-network-based approaches which are more comparable to GAN-based approaches. We then look at the recent adversarial domain adaptation methods which are inspired by GANs. Tables 1 and 2 summarize the neural network-based methods we discuss (both non-adversarial and adversarial). Additionally, Tables 3 through 6 summarize the results of evaluating many of these methods on datasets used in the domains of image processing as well as sentiment analysis.

4.1 Non-Adversarial Domain Adaptation

4.1.1 Without neural networks. Daumé [23] lists six “obvious” domain adaptation methods that perform fairly well in the semi-supervised case. A “source only” model is trained only on the source data. Similarly, a “target only” model is trained only on the target data and an “all” model is trained on the union of both. In contrast, a “weighted” model uses both data sources but weights (chosen by cross validation) source and target data differently to even out the imbalance. A “prediction” model uses the output of the “source only” model as additional features for learning on the target data. Finally, a “linearly interpolated” model linearly interpolates between “source only” and “target only” models.

Daumé [23] also describes two methods that outperform the above six baselines. First, the “prior” model uses the “source only” output as a prior for the weights of another model trained on the target data. Rather than regularizing the target model weights with an L2 norm, which prefers smaller magnitude weights, the model instead prefers weights similar to that of the source model unless the target data strongly suggests otherwise. For example, if one of the source weights was 5, then the corresponding target weight would be regularized to be near 5 rather than 0 as it would if using an L2 norm. Second, another option is to use three models for different types of information: source-specific, target-specific, and general. Each source example is either source-specific or general,

Table 1. Comparison of different neural network based domain adaptation methods.

| Name | Adaptation | | Loss Functions | | | | | | Adversarial Loss | | Gen. | Shared |
|--------------------------------|------------|-------|----------------|-------|-------|----------|-----------|------|------------------|-------|------|------------------|
| | Feature | Pixel | Distance | Diff. | Cycle | Semantic | Pix. Sim. | Task | Feature | Pixel | | |
| CyCADA[53] | ✓ | ✓ | | | ✓ | ✓ | | ✓ | ✓ | ✓ | ✓ | |
| Rozantsev et al.[106] | ✓ | | MMD | | | | | ✓ | | | | ^a |
| PixelDA[15] | | ✓ | | | | ✓ | ✓ | ✓ | | ✓ | ✓ | ✓ |
| VADDA[100] ^b | ✓ | | | | | | | ✓ | ✓ | | | ✓ |
| Saito et al.[109] | ✓ | | | ✓ | | | | ✓ | | | | low |
| SimGAN[112] | | ✓ | | | | | ✓ | | | ✓ | ✓ | N/A ^c |
| ADDA[119] | ✓ | | | | | | | ✓ | ✓ | | | |
| CycleGAN[129] | | ✓ | | | ✓ | | | | | ✓ | ✓ | ^d |
| DSN[16] | ✓ | | ^e | ✓ | ✓ | | | ✓ | ✓ | | | some |
| DRCN[43] | ✓ | | | | ✓ | | | ✓ | | | | ✓ |
| CoGAN[72] | ✓ | | | | | | | ✓ | ✓ | | ✓ | some |
| Deep CORAL[115] | ✓ | | CORAL | | | | | ✓ | | | | ✓ |
| DANN[37, 38] | ✓ | | | | | | | ✓ | ✓ | | | ✓ |
| DAN[75] | ✓ | | MK-MMD | | | | | ✓ | | | | low |
| Tzeng et al.[118] ^f | ✓ | | | | | | | ✓ | ✓ | | | ✓ |

^ano sharing of weights, but regularized to be similar

^buses a variational RNN [20] rather than a CNN because applying to multimodal sequential (time series) data

^cmaps to target domain so only have feature extractor for target (part of the classifier)

^dunspecified; originally not applied to domain adaptation, but Hoffman et al. [53] tried it

^etried MMD but found adversarial performed better

^fsemi-supervised for some classes, i.e. requires some labeled target data for some of the classes

and each target example is either target-specific or general. A previous paper [24] proposed an EM algorithm for training but it was 10-15 times slower than the “prior” model training.

Finally, Daumé proposes a method that is “frustratingly easy” and trains much faster. Instead of each *example* being one of the three cases, now each *feature* of the data is either source-specific, target-specific, or general. The data will be augmented so the source data will have source-specific and general features (target-specific is zeros) and the target data will have target-specific and general features (source-specific is zeros). The input data (either target or source) is duplicated into both the specific and general features of each example. In other words, source data will be $\langle x, x, 0 \rangle$ and target data $\langle x, 0, x \rangle$, where 0 is a vector of length $|x|$ and x is each example’s original data. A kernelized version is also described which replaces x with the function $\Phi(x)$. The method can be extended to process multiple source domains and has been evaluated on sequence labeling tasks.

4.1.2 With neural networks. More recently much work has focused on neural network methods that do not require any labeled target data, i.e. unsupervised domain adaptation. Long et al. [75] introduce deep networks for domain adaptation in this unsupervised case, called deep adaptation networks (DAN). Previous methods learned shallow features by minimizing a distance between domains, but deep networks are superior at representing hierarchical features and identifying features invariant to noise. However, the higher layers do not transfer well between domains. Long et al. copy the lower layers and adapt the higher layers rather than the more simple approach of copying the lower layers and fine-tuning the network again with a small amount of labeled target data, which allows their method to not require any labeled target data and also be less likely to overfit [75]. To adapt the layers, they use the multiple kernel variant maximum mean discrepancy

Table 2. Terms used for comparing neural network based domain adaptations in Table 1.

| Explanation of Comparison Terms | |
|---------------------------------|---|
| Adaptation | either feature-level or pixel-level (raw input) adaptation (or both) |
| Loss Functions | Distance – trying to align distributions through minimizing a distance function |
| | Diff. – enforce different features between two networks, e.g. learning separate private and shared features |
| | Cycle – cycle consistency (reconstruction) loss |
| | Semantic – semantic consistency loss (same label before and after pixel-level translation) |
| | Pix. Sim. – pixel-level similarity loss |
| | Task – task loss, e.g. if for classification, outputting the groundtruth source label, or if for semantic segmentation, labeling each pixel with the correct groundtruth source label |
| Adversarial Loss | adversarial loss performed on either feature-level output or pixel-level output (or both); note that the difference between an “adversarial loss” and the “loss functions” above is that the loss functions above are generally a more simple equation whereas the adversarial loss is a learned neural-network discriminator trained to not be able to distinguish between two (or more) domains, i.e. a learned loss function (where learning is more than a hyperparameter search) |
| Gen. | uses a generator during training |
| Shared | encoders share weights, i.e. sharing weights between the source and target feature extractors |

Table 3. Classification accuracy (source \rightarrow target, mean \pm std %) of different neural network based domain adaptation methods on various computer vision datasets (only including those used in > 2 papers). Adversarial approaches denoted by *.

| Name | MNIST and USPS | | MNIST and SVHN | | MNIST[-M] | Synthetic to Real | |
|---|----------------------------------|---------------------|--|---------------------|--------------------------------------|-----------------------------------|--------------------------------------|
| | MN \rightarrow US | US \rightarrow MN | SV \rightarrow MN | MN \rightarrow SV | MN \rightarrow MN-M | SYN _N \rightarrow SV | SYN _S \rightarrow GTSRB |
| Target only (i.e., if we had the target labels) | 96.3 \pm 0.1 [53] 96.5 [15] | 99.2 \pm 0.1 [53] | 99.2 \pm 0.1 [53] 99.5 [16] 99.51 [37] | | 96.4 [15] 98.7 [16] 98.91 [37] | 92.44 [37] 92.4 [16] | 99.87 [37] 99.8 [16] |
| CyCADA[53]* | 95.6 \pm 0.2 | 96.5 \pm 0.1 | 90.4 \pm 0.4 | | | | |
| Rozantsev et al.[106] | 60.7 | 67.3 | | | | | |
| PixelDA[15]* | 95.9 | | | | 98.2 | | |
| Saito et al.[109] | | | 85.0 | 52.8 | 94.0 | 92.9 | 96.2 |
| ADDA[119]* | 89.4 \pm 0.2 | 90.1 \pm 0.8 | 76.0 \pm 1.8 | | | | |
| DSN[16] ^d * | 91.3 [15] | | 82.7 | | 83.2 | 91.2 | 93.1 |
| DRCN[43] | 91.80 \pm 0.09 | 73.67 \pm 0.04 | 81.97 \pm 0.16 | 40.05 \pm 0.07 | | | |
| CoGAN[72]* | 91.2 \pm 0.8 | 89.1 \pm 0.8 | | | 62.0 [15] | | |
| DANN[37, 38]* | 85.1 [15] | | 71.07 70.7 [16] 71.1 [109] 73.6 [53] | 35.7 [109] | 81.49 77.4 [16] 81.5 [109] | 90.48 90.3 [16, 109] | 88.66 88.7 [109] 92.9 [16] |
| DAN[75] | 81.1 [15] | | 71.1 [16] | | 76.9 [16] | 88.0 [16] | 91.1 [16] |
| Source only (i.e., no adaptation) | 78.9 [15] 82.2 \pm 0.8 [53] | 69.6 \pm 3.8 [53] | 59.19 [37] 59.2 [16] 67.1 \pm 0.6 [53] | | 56.6 [16] 57.49 [37] 63.6 [15] | 86.65 [37] 86.7 [16] | 74.00 [37] 85.1 [16] |

^dresults using adversarial loss, which are higher than those using MMD; also used some target labels in validation data for hyperparameter tuning

Table 4. Classification accuracy (source \rightarrow target, mean \pm std %) of different neural network based domain adaptation methods on the Office computer vision dataset. Adversarial approaches denoted by *.

| Name | Office (Amazon, DSLR, Webcam) | | | | | |
|--------------------------------------|-------------------------------|-------------------------|-------------------------|----------------------|----------------------|----------------------|
| | A \rightarrow W | D \rightarrow W | W \rightarrow D | W \rightarrow A | A \rightarrow D | D \rightarrow A |
| Rozantsev et al.[106] | 76.0 | 96.7 | 99.6 | | | |
| ADDA[119]* | 75.1 | 97.0 | 99.6 | | | |
| DRCN[43] | 68.7 \pm 0.3 | 96.4 \pm 0.3 | 99.0 \pm 0.2 | 54.9 \pm 0.5 | 66.8 \pm 0.5 | 56.0 \pm 0.5 |
| Deep CORAL[115] | 66.4 \pm 0.4 | 95.7 \pm 0.3 | 99.2 \pm 0.1 | 51.5 \pm 0.3 | 66.8 \pm 0.6 | 52.8 \pm 0.2 |
| DANN[37, 38]* | 67.3 \pm 1.7 | 94.0 \pm 0.8 | 93.7 \pm 1.0 | | | |
| | 72.6 \pm 0.3 [43] | 96.4 \pm 0.1 [43] | 99.2 \pm 0.3 [43] | 52.7 \pm 0.2 [43] | 67.1 \pm 0.3 [43] | 54.5 \pm 0.4 [43] |
| | 73.0 [106, 119] | 96.4 [106, 119] | 99.2 [106, 119] | | | |
| DAN[75] | 68.5 \pm 0.4 | 96.0 \pm 0.3 | 99.0 \pm 0.2 | | | |
| | 63.8 \pm 0.4 [115] | 94.6 \pm 0.5 [115] | 98.6 [106] | 53.1 \pm 0.3 | 67.0 \pm 0.4 | 54.0 \pm 0.4 |
| | 64.5 [106] | 95.2 [106] | 98.8 \pm 0.6 [115] | 51.9 \pm 0.5 [115] | 65.8 \pm 0.4 [115] | 52.8 \pm 0.4 [115] |
| | 68.5 [119] | 96.0 [119] | 99.0 [119] | | | |
| Tzeng et al.[118] ^{a*} | 59.3 \pm 0.6 | 90.0 \pm 0.2 | 97.5 \pm 0.1 | 40.5 \pm 0.2 | 68.0 \pm 0.5 | 43.1 \pm 0.2 |
| Source only (i.e., no adaptation) | 62.6 [119] ^b | 96.1 [119] ^b | 98.6 [119] ^b | | | |

^asemi-supervised for some classes, but evaluated on 16 hold-out categories for which the labels were not seen during training

^bOffice dataset numbers are using a ResNet-50 network though Tzeng et al. [119] also provided AlexNet results

Table 5. Classification accuracy comparison for domain adaptation methods for sentiment analysis (positive or negative review) on the Amazon review dataset [13] ^a. Adversarial approaches denoted by *.

| Source | Target | DANN mSDA[38] ^{b*} | DANN[38] ^{c*} | CORAL[114] ^d | No Adaptation[114] ^e |
|-------------|-------------|-----------------------------|------------------------|-------------------------|---------------------------------|
| Books | DVD | 82.9 | 78.4 | | |
| Books | Electronics | 80.4 | 73.3 | 76.3 | 74.7 |
| Books | Kitchen | 84.3 | 77.9 | | |
| DVD | Books | 82.5 | 72.3 | 78.3 | 76.9 |
| DVD | Electronics | 80.9 | 75.4 | | |
| DVD | Kitchen | 84.9 | 78.3 | | |
| Electronics | Books | 77.4 | 71.3 | | |
| Electronics | DVD | 78.1 | 73.8 | | |
| Electronics | Kitchen | 88.1 | 85.4 | 83.6 | 82.8 |
| Kitchen | Books | 71.8 | 70.9 | | |
| Kitchen | DVD | 78.9 | 74.0 | 73.9 | 72.2 |
| Kitchen | Electronics | 85.6 | 84.3 | | |

^a<http://www.cs.jhu.edu/~mdredze/datasets/sentiment/>

^busing 30,000 dimensional feature vectors from marginalized stacked denoising autoencoders (mSDA) by Chen et al. [18], which is an unsupervised method of learning a feature representation from the training data

^cusing 5000-dimensional unigram and bigram feature vectors

^dusing bag-of-words feature vectors including only the top 400 words, but suggest using deep text features in future work

^eusing bag-of-words feature vectors

Table 6. List and description of computer vision datasets from Tables 3 and 4

| Computer Vision Datasets used for Domain Adaptation | |
|---|--|
| MNIST [69] ^a | This is a binary (mostly black and white, but actually grayscale due to anti-aliasing) handwritten digit dataset (digits 0-9), which stands for “modified NIST.” It is based on the National Institute of Standards and Technology’s (NIST) Special Database 1 and 3, one of which was easier than the other, so MNIST is a combination of the two that are size normalized to fit in a 20x20 box preserving the aspect ratio and centered in a 28x28 pixel image. |
| MNIST-M [38] ^b | This is a modification of MNIST where the digits are blended with random patches from BSDS500 dataset color photos. |
| USPS [70] ^c | This is another handwritten digit dataset (digits 0-9). It consists of handwritten zipcodes scanned and segmented by the U.S. Postal Service (USPS). They were size normalized to 16x16 pixels preserving the aspect ratio. The values are normalized to be between -1 and 1. |
| SVHN [88] ^d | The Streetview House Numbers (SVHN) consists of single digits extracted from images of urban house numbers in Google Street View. The digits have been size normalized to 32x32 pixels. |
| SYN_N [38] ^b | Ganin et al. [38] used Microsoft Windows fonts to create a synthetic digit dataset (“Syn Numbers”) consisting of 1-3 digit numbers with various positions, orientation, background color, stroke color, and amount of blur. |
| SYN_S [86] ^e | This is a synthetic sign dataset created from modifications to Wikipedia pictograms of traffic signs. It consists of 100,000 images and 43 classes of signs. |
| GTSRB [113] ^f | The German Traffic Signs Recognition Benchmark (GTSRB) is a dataset created from video taken driving around Germany. It consists of about 50,000 images and 43 classes of signs. |
| Office [108] ^g | This dataset consists of 31 classes of objects in three different domains: Amazon (taken from its online website; medium resolution and studio lighting), DSLR (taken with a digital SLR camera; high resolution and in a real-world environment), and Webcam (taken with a 640x480 computer webcam; have noise, artifacts, and white balance issues). Note: due to Office’s small size, some networks [38, 106, 115] were pre-trained on ImageNet. |

^a<http://yann.lecun.com/exdb/mnist/>

^bSee Ganin’s website <http://yaroslav.ganin.net/> for links to download.

^cThis can be found on various sites and some Github repositories. One such place:

<https://web.stanford.edu/~hastie/ElemStatLearn/data.html>

^d<http://ufldl.stanford.edu/housenumbers>

^eThe synthetic dataset linked to on: <http://graphics.cs.msu.ru/en/research/projects/imagerecognition/trafficsign>

^f<http://benchmark.ini.rub.de/?section=gtsrb&subsection=dataset>

^g<http://ai.bu.edu/adaptation.html>

(MK-MMD) to minimize the discrepancy between source and target domains. By adapting multiple layers, they can overcome the source and target dataset bias [75].

Ghifary et al. [43] hypothesize that unsupervised domain adaptation can be accomplished by learning a representation that both classifies the labeled source domain data well and reconstructs the unlabeled target domain data. To do this they introduce deep reconstruction-classification networks (DRCN). For source domain classification, they utilize a feature extraction network followed by a fully-connected layer and softmax layer to output source class labels. For reconstruction of the

target image from the learned representation by the feature extractor, the feature extraction network is followed by a reconstruction network, which rather than downsampling with max-pooling (as in the feature extractor) instead upsamples by duplicating the pooled values to the additional locations in the feature map. Classification of the labeled source domain data trained with cross-entropy loss is alternated with reconstruction of the unlabeled target data trained with a pixel-wise squared loss.

Saito et al. [109] propose an alternative method for unsupervised domain adaptation using three networks. Two networks are trained on the labeled source data. Those two networks then predict the labels for the unlabeled target data, and if the two agree on the label and have high enough confidence on a particular instance, then the predicted label for that example is assumed to be the true label. After the target data is labeled by the first two networks, the third network can be trained using the assumed-true labels. The three networks share weights for the first portion of the network, the feature extractor, and the two labeling unlabeled target data are trained with a loss such that they learn to make predictions using different features.

Recall from Section 3.2 that target error is upper bounded by the sum of the source error, $\mathcal{H}\Delta\mathcal{H}$ -divergence, and the ideal predictor error λ . This is different from other methods like Long et al. [75] and Ganin et al. [37] (will be discussed in Section 4.2), which focused on minimizing the middle term using a divergence measure and assume λ is small, since Saito et al. instead focused on minimizing an approximation of the λ term using the assumed-true labels.

Another unsupervised non-adversarial method continues in the line of “frustratingly easy” domain adaptation methods (though those were semi-supervised), only requiring 4 lines of code in Matlab to implement. To align the source and target distributions, CORAL by Sun et al. [114] computes the covariance for each domain and adds a whitening and re-coloring linear transform step for the source data before training a source classifier. They additionally proposed Deep CORAL [115] for integrating into deep neural networks.

4.2 Adversarial Domain Adaptation

Recall that generative adversarial networks (GANs) include a discriminator that tries to accurately predict whether a sample is from the real data distribution or from the generator. In other words, the discriminator differentiates between two distributions, one real and one fake. This discriminator could similarly be set up such that the two distributions to differentiate instead represent a source distribution and a target distribution. Such a process could be used to train a deep neural network that performs well in the target domain. This is the process of adversarial domain adaptation.

In exploring this idea we first consider adaptation at the feature level, meaning there is a feature extractor (encoder) that creates a feature representation and during training adjusts that representation to work well for both source and target domains. This adaptation contrasts with pixel-level adaptation, in which the raw input (in this case pixels) is mapped from the source domain to the target domain, making the input image look like a target image. Figure 8 shows an example of adapting a synthetic vehicle-driving image at a pixel level to look realistic.

4.2.1 Feature-Level Adaptation. The unsupervised domain adaptation setup in Ganin et al. [37, 38], called a domain-adversarial neural network (DANN), consists of three components: a feature extractor network, a label predictor network, and a domain classifier network. The feature extractor accepts as input data from either the source or target domain and creates a feature vector as output. The label predictor accepts this feature vector and predicts the class label. The domain classifier also accepts the same feature vector and determines whether the data came from the source or target domains.

During training, first the feature extractor followed by the label predictor is trained on all of the source data. Next, the feature extractor followed by the domain classifier is trained on both source and target data since it does not require labels. Finally, the feature extractor followed by the label predictor is applied to the target data for testing. The goal is for the feature extractor network is to learn domain-invariant features, i.e. features that allow for high classification accuracy on both the source and target domains. If the feature distribution output by the feature extractor is different between source and target, then the domain classifier will be able to distinguish them. Thus, through adversarial training, the feature extractor will be forced to align the feature vector distributions between source and target domains.

Ganin et al. [37] introduce a gradient reversal layer, which multiplies the gradient by a small negative number, to train the feature extractor to prevent the domain classifier from being able to discriminate between source and target domains. In other words, the feature extractor is trained to *maximize*, not minimize, the domain classifier’s loss. Without this layer, during training the feature extractor would learn features that would be distinguishable, which is the opposite of the goal.

Tzeng et al. [118] consider a similar setup for semi-supervised domain adaptation. By incorporating some labeled target examples and matching label distributions they were able to improve the earlier results. Rather than including a gradient reversal layer to directly maximize the domain classifier’s loss, they instead maximize domain confusion to “maximally confuse” the domain classifier. The domain classifier is “maximally confused” when it outputs a uniform distribution over binary labels, which indicates that the domain classifier cannot determine whether the learned feature representation of an input image is from the source or target domain. Because they require some labeled target examples, they match the label distributions, or enforce that the relationships between the classes in the source domain carry over to the target domain. For example, they note that a bookshelf is more similar to a filing cabinet than a bike, which represents a relationship that would be preserved in the target model.

Ganin et al. [37] use the exact same feature extractor on both the source and target domains, and with the same effect Tzeng et al. [118] share the feature extractor weights. Having two separate source and target networks that share all of their weights is equivalent to using the same network for both domains, but separate networks offer fine-grained control over which layers share weights. In contrast to Ganin et al. and Tzeng et al., Rozantsev et al. [106] show that it is better to not share weights and instead introduce a regularizer that keeps the weights somewhat similar but does not penalize linear transformations of the weights in corresponding layers. While this offers an improvement for adaptation, Rozantsev et al. did not use an adversarial approach. The idea of regularizing to the source weights is similar to the “prior” method discussed in Section 4.1.

Bousmalis et al. [16] propose another variant to the idea of sharing (or not sharing) weights called domain separation networks (DSN). Similar to Daumé’s [23] method of including general (here called “shared”) or domain-specific features, Bousmalis et al. also learn source-specific, target-specific, and shared features. Unlike Daumé, this method does not require any labeled target data. This approach can thus be classified as unsupervised domain adaptation, although they use labeled target data for hyperparameter tuning. Here the “shared” source domain encoder and “shared” target domain encoder do share weights, but the “private” source domain encoder and “private” target domain encoders do not. The best performance is achieved by applying an adversarial loss rather than maximum mean discrepancy (MMD) for enforcing similarity between the shared encoder outputs. For enforcing different private features, a soft subspace orthogonality constraint can be applied.

Unlike their 2015 paper, Tzeng et al. [119] do not require labeled target data (i.e. this later paper is unsupervised) in adversarial discriminative domain adaptation (ADDA), and they follow Rozantsev et al. [106] in not requiring shared weights. A two-step training method is proposed. First, a source

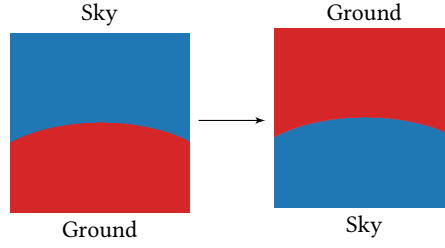


Fig. 9. Example semantic segmentation situation in which the class names are swapped between the input image and the mapped image that would be prevented by including a semantic-consistency loss. The semantic-consistency loss requires that the class assignments are preserved.

encoder (feature extractor) is trained on the source data, followed by training a source classifier (label predictor) on the source data. Second, a target encoder is trained such that a discriminator cannot distinguish between the source and target domains using the target encoder's and source encoder's outputs. During this second training step, only the target encoder and discriminator weights are updated but not the weights of the source encoder. Note that the training is performed by inverted labels rather than a gradient reversal layer. Finally, they test using the target encoder followed by the source classifier.

The above approaches focus on learning from non-sequential data. In the case of sequential or time-series data, such as learning temporal latent relationships in health data across different population age groups, Purushotham et al. [100] propose variational adversarial deep domain adaptation (VADDA). VADDA uses a variational RNN [20] rather than a CNN. The variational RNN learns the temporal relationships while using adversarial training to achieve domain adaptation.

An alternative to training purely for a discriminative task in the target domain is to generate data as in a GAN. One such generator is CoGAN, created by Liu et al. [72]. They train a pair of GANs on two domains. Here, the first few layers of the generators and the last few layers of the discriminators share weights. A softmax layer is added to the last hidden layer of the source discriminator, which enables predicting the label (e.g. digits if trained on MNIST) of both real and fake input images. The source and target GANs are trained with the images in source and target domains respectively while simultaneously training the softmax layer of the source GAN to output the correct source image label. During testing, the target discriminator is employed with a softmax layer after the last hidden layer for classification. Note that Tzeng et al. [119] had difficulty making this method converge for larger shifts between source and target.

4.2.2 Pixel-Level Adaptation. Another way of using a generator is with a conditional GAN. This results in the generator performing adaptation at the pixel level, i.e. translating a source input image to an image that matches the target distribution. Then a classifier could be trained on the source data mapped to the target domain using the known source labels. This is a possible setup for using CycleGAN [129]. Though the original CycleGAN paper was application agnostic, Hoffman et al. [53] experimented applying it to domain adaptation, but they found their method outperformed using CycleGAN, which will be discussed in Section 4.2.3.

In pixel-level domain adaptation (PixelDA), Bousmalis et al. [15] also used a conditional generator to map from the source domain to the target domain. The generator took as input both a source domain example (synthetic images in their examples) and a noise vector (which CycleGAN did not have), allowing for easy data augmentation by changing the noise vector. Then, both the original source image and the output of the generator were fed to a classifier, which helped with

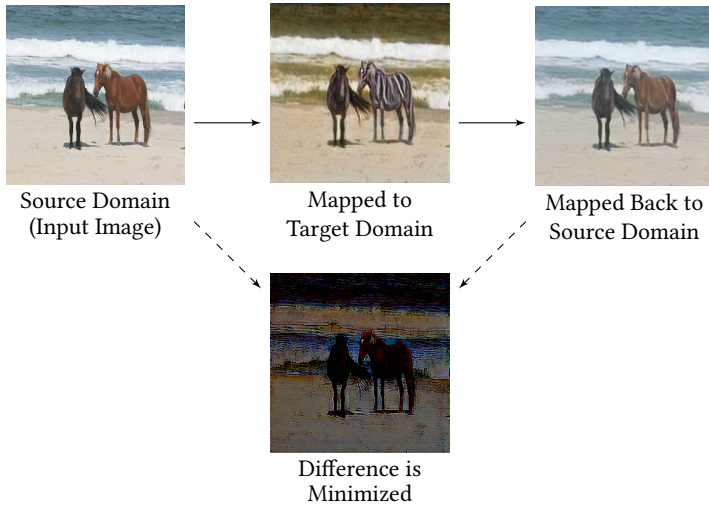


Fig. 10. Illustration of a cycle-consistency loss using the horses \leftrightarrow zebras dataset by Zhu et al. [129]. The difference between the original source image and the reconstructed image (source to target and back to source) is minimized.

stabilizing training and preserving class assignments (e.g. source class 1 does not end up being “renamed” target class 2, see Figure 9). Finally, the output of the generator and the unlabeled target examples were fed to a discriminator to force the generator to match the target domain distribution (adversarial training). Because they were using synthetic images and knew which pixels were foreground in these images, they additionally introduced a content-similarity loss penalizing only foreground pixel differences. The main downside to their approach is that they state that their method assumes that the domain difference is primarily low level.

Shrivastava et al. [112] (SimGAN) also investigate pixel-level adaptation. Similar to Bousmalis et al. [15] they use a pixel-level similarity loss (similar to the content-similarity loss) but apply L1 with a transformation function (e.g. identity, image derivatives, mean of color channels, etc.). They first tested an adversarial loss via a discriminator but found that instead using a *local* adversarial loss (discriminator which only looks at small region of pixels) reduced artifacts. Finally, rather than using only the latest generated images in a minibatch, the discriminator makes its decision on a mix of the current batch of generated images and some from a history of past generated images, which reduces the likelihood that artifacts will return.

4.2.3 Feature-level and Pixel-level Adaptation. Another option is to perform both feature-level and pixel-level adaptation, which Hoffman et al. [53] found to significantly improve unsupervised domain adaptation accuracy, particularly for larger domain shifts than what Bousmalis et al. [16] and other pixel-level image translation methods can support. Domain adaptation methods only adapting at the feature level may not properly adapt lower level domain shifts such as at the pixel level. Thus, they try performing first pixel-level adaptation followed by feature-level adaptation. This combination offers the added benefit of being able to visually inspect the pixel-level adapted results as a sanity check.

These authors employ a cycle consistency loss, a semantic consistency loss, GAN losses, and a task loss. They call this method cycle-consistent adversarial domain adaptation (CyCADA). The cycle consistency loss requires that not only can the conditional generator map from the source

to target domain but also using another generator subsequently map back from the target to the source domain to reconstruct the original input as illustrated in Figure 10. Similarly, another loss is for the target to source and back. In other words, a cycle consistency loss is a reconstruction loss [53]. The cycle consistency loss is included so as to not require a correspondence between source and target domain images in the training data. Like in PixelDA, semantic consistency is enforced to preserve class assignments as illustrated in Figure 9. The semantic consistency loss requires that a classifier output (or semantic segmentation labeling) from the original source image is the same as the same classifier’s output on the pixel-level mapped target output. An adversarial (“GAN”) loss is used at the pixel-level to prevent the discriminator from distinguishing between the source and target domains. Another adversarial loss is used at the feature level, similarly to prevent distinguishing between the domains. Finally, the task loss is based on the desired task, e.g. to minimize image classification or segmentation error.

To train a model with so many components, they trained it in stages. First, they trained the source feature extractor and classifier with the task loss. Second, they trained the generators (source to target and target to source) and pixel-level discriminators using the cycle consistency loss, semantic consistency loss, and pixel-level GAN loss. Simultaneously they trained an initial target feature extractor and classifier with the source images mapped to the target domain and the corresponding source labeled data. Finally, they updated the target feature extractor and classifier with the feature-level GAN loss.

4.3 Ongoing Research

The more difficult domain adaptation problems are far from being solved. Tables 3 through 6 indicate that some domain adaptation problems are harder than others and point to the challenge that more work needs to be focused on these harder problems. While accuracy for SVHN→MNIST ranges from 70.7% to 90.4%, for the reverse case of MNIST→SVHN, the highest is 52.8% by Saito et al. [109]. This reverse problem is much harder [37]. As a result, few papers offer results for this direction and continued work is needed to strengthen bi-directional adaptation.

However, recent approaches have improved accuracy in some of these adaptation problems using GANs or GAN-inspired adversarial losses. For example, by utilizing pixel-level adaptation with a GAN, PixelDA obtains the highest accuracy on MNIST→MNIST-M (Table 3). By using an adversarial loss rather than MMD, Bousmalis et al. [16] increase the accuracy of DSN across a variety of datasets. CyCADA increases accuracy from 54% to 82% for a synthetic season adaptation dataset [53], from 90.1% to 96.5% on USPS→MNIST, and from 85.0% to 90.4% on SVHN→MNIST (Table 3) by incorporating pixel-level adaptation using a GAN to perform image-to-image translation in addition to feature-level adaptation, both of which include adversarial losses. These improvements indicate that GANs or GAN-inspired adversarial losses may be a key ingredient in solving additional domain adaptation problems such as the more-difficult MNIST→SVHN.

5 RESEARCH DIRECTIONS

As we have seen, the rapidly-growing body of research focused on generative adversarial networks now encompasses several novel approaches to domain adaptation. Here we look at what could be explored in future research to further enhance this existing work.

5.1 GANs

5.1.1 Training and Evaluation. As mentioned in Sections 2.3 and 2.4, there is room for work in GAN training and evaluation. GANs can encounter many training issues such as mode collapse, vanishing gradients, and non-convergence. While an approximate Nash equilibrium does exist for some GAN objective functions (e.g. Wasserstein), whether GAN training can find this equilibrium

using backpropagation is an open problem [4]. Further work can be done to address these issues. Another potential problem for neural network training was discovered by Balduzzi et al. [7]. This is the “shattered gradient” problem, which is why residual networks with skip connections so effectively handle very deep networks. They propose an alternate initialization method to prevent shattering and not require skip connections. This could be investigated for GANs as well, which might allow for training deeper networks as well.

In addition, it is difficult to evaluate GANs due to each evaluation method giving an incomplete picture and many requiring human involvement. Sample inspection for visual quality and the birthday paradox test for determining diversity both require human involvement, whereas automated metrics such as FID and approximate log-likelihoods do not always correlate with the visual quality of samples. Given a particular use case for GANs, it may be possible to use a task-based method for evaluation. For example, classification accuracy is used for domain adaptation evaluation since in this problem the end goal is performance on a particular target domain.

5.1.2 Applying Adversarial Losses. Recall in Section 2.1 that the discriminator can be thought of as learning a loss function to discriminate between real and fake data, rather than specifying a simpler loss like mean-squared error, which resulted in blurry images, or a human perception loss, which is harder to define. This is the idea carried over to adversarial domain adaptation with “adversarial loss” functions discussed in Section 4.2, except that in domain adaptation the network discriminates between source and target domains rather than real vs. fake data. Learning a loss function facilitates enforcing a higher-level and easier-to-specify goal, in this case not wanting the domains to be distinguishable. The key here is that distinguishing domains is a classification problem, and there has been much success in machine learning-based classification. Thus, now we want to *not* be able to learn a neural network to be good at classifying by domain. Then the gradients can be used to update the model (whether a generator, feature extractor, or some other network).

The exact same adversarial loss can be applied in other areas with the goal of not wanting to be able to distinguish between two items, but this idea could also be applicable in contexts with other high-level goals. For example, one goal might be training to not be able to learn how to compress (e.g. not be able to learn an autoencoder with low reconstruction loss) or linearly separate (e.g. not be able to learn to classify using a perceptron). While these may not be particularly useful objectives (use entropy for not being able to compress and apply a non-linear function to not be able to linearly separate), they demonstrate the possibility of specifying alternate high-level objectives for an adversarial loss.

The various problems mentioned in Section 2.5 offer useful high-level goals. In the adversarial spatial dropout and transformer networks by Wang et al. [121], the adversarial network generates partially occluded or transformed examples that the current model has a hard time getting correct. In the shaking and snatching robot grasping adversaries by Pinto et al. [99], the adversary tries to learn to behave (either through shaking or snatching) such that the robot cannot grasp the object. This GAN-inspired idea of adversarial losses can be applied to a wide range of problems.

5.2 Domain Adaptation

5.2.1 Hyperparameter Tuning. Normal supervised learning-based hyperparameter tuning methods do not carry over to unsupervised domain adaptation. A common supervised learning approach is to split the training data into a smaller training set and a validation set. After repeatedly altering the hyperparameters, retraining the model, and testing on this validation set for each set of hyperparameters, the model yielding the highest validation set accuracy is selected. Another option is cross validation. However, in unsupervised domain adaptation, there are now two domains, and the data

for the target domain may not include any labels. When evaluating domain adaptation approaches on common datasets, generally the target data contains labels, so work by groups such as Bousmalis et al. [16] does use some labeled target data for hyperparameter tuning. This is not ideal because real-world testing will not include labels for tuning (unless it is semi-supervised, in which case semi-supervised learning is recommended in Section 3.2). A hyperparameter methodology may be developed that does not require labeled target data.

5.2.2 *Balancing Classes.* Hoffman et al. [53] noted that the frequency-weighted intersection over union results in their paper were very close to the target-only model accuracy (an approximate upper bound). Thus, they concluded that their pixel-level adaptation followed by feature-level adaptation is very effective for the common classes in the SYNTHIA dataset (season adaptation on a synthetic driving dataset). It is possible then that additional balancing of classes could help the not-as-common classes to perform better. In addition, data augmentation through occluding parts of the images may improve class balancing as would the adversarial spatial dropout network by Wang et al. [121] since the two best classes (road and sky) were likely in almost every image.

5.2.3 *Applying to Smart Homes.* A commonly-addressed application of domain adaptation is in computer vision, the primary application discussed in Section 4.2. Another is in natural language processing such as sequence labeling in Daumé’s work [23] and sentiment analysis performed by Sun et al. [114] and Ganin et al. [38]. A promising application area that has not been explored is smart home data generation and adaptation.

If a smart home contains cameras, then the existing techniques applied to computer vision that were discussed in Section 4.2 could be used. However, some smart homes employ sensors other than image data, including passive infrared motion sensors, door open/closed sensors, light sensors, and temperature sensors [21]. Other behavioral monitoring systems utilize RFID tags and mobile devices (such as smart phones or smart watches) [67]. With these various sensors and setups, given a model for some task such as activity recognition trained on one set of sensors (e.g. RFID), it may be beneficial to adapt the model to be used on other sensors (e.g. motion sensors). For instance, the activity recognition models that have been developed for smart homes [65] could potentially be adapted to operate on data from another set of sensors, e.g. a different smart home setup or a smart watch.

Often in the computer vision context the same labels and feature spaces are used in both the source and target domains. The smart homes may be more difficult due to changes in activity labels between different smart home models. For example, one model may learn the “walk” activity while another learns “exercise” or may learn “read” while another similar model learns “school” (reading may be for education or for enjoyment). Similarly, models may need to adapt to different sensor modalities, e.g. switching from images to mobile device motion or to ambient sensors such as infrared motion detectors.

Some of the ideas from current domain adaptation methods could potentially be used for adapting models across sensor modalities for smart homes. Aytaç et al. [6] performed unsupervised transfer learning across modalities: vision to sound. CoGAN [72] was used to generate correspondences between color and depth images. This could be applied to generate correspondences across modalities (e.g. a vector of accelerometer readings from a mobile phone may correspond to a vector of smart home motion sensor readings). CyCADA [53] suggests performing pixel-level then feature-level adaptation. Maybe this process could be modified to first transfer to the other modality (rather than the pixel-level adaptation step) and then perform feature-level domain adaptation in the other modality. With various methods, synthetic data via 3D renderers have been combined with domain adaptation to improve accuracy. Synthetic data could similarly be used in a smart home setting. This

may particularly be helpful if the synthetic data could be generated for multiple sensor modalities (with or without correspondence).

Smart homes also offer a temporal aspect. In a computer vision context, the networks are generally run on a single image frame (though there are a few video-based networks [6, 27, 120]). In a smart home context, there may be a stream of sensors turning on and off over a period of time. In order to make any activity predictions, this stream of sensor events must be interpreted. A combination of CNNs and RNNs have been used in domain generalization for handling a radio spectrogram changing through time to identify sleep stages [128]. Variational adversarial deep domain adaptation (VADDA), which uses variational RNNs, was proposed by Purushotham et al. [100] for learning temporal latent relationships in health data across different age groups of people. Possibly VADDA or a combination of CNNs and RNNs could similarly be applied in a smart home context to handle these streams of sensor events.

5.3 Other Problems

Adversarial techniques could be applied to machine learning security, where the goal is to train a classifier robust to adversarial examples [55]. From a GAN discriminator's perspective, the generator is an adversary trying to cause the discriminator to make an incorrect classification. Through the GAN adversarial training process, the discriminator is able to decrease classification error. A GAN might similarly be used to generate adversarial examples to make a classifier more robust.

6 CONCLUSIONS

GANs are a popular new method. In this paper we review various interpretations of GANs including generative modeling, density estimation, energy function learning, and reinforcement learning. We observe that GANs can be difficult to train and to evaluate in a human-free manner. Once trained, GANs have been able to produce amazingly realistic images.

In addition, we highlight the fact that ideas stemming from GANs such as adversarial losses are spreading to other problems, including domain adaptation. Building on prior GAN research, theories are now offered that provide upper bounds on target error given the source error, domain divergence, and ideal predictor error. Many non-adversarial and adversarial methods investigate domain adaptation at either the feature level, pixel level, or both. These have been tested and compared on a variety of datasets.

Moving forward, we point out the observation that continuing work is needed to improve GAN training and evaluation. Similarly, there is room for much more research applying GAN ideas to other problems like transfer learning. The power of GANs for domain adaptation and transfer learning offers strategies that, if harnessed, can tackle difficult problems in image processing, natural language processing, and emerging applications in human behavior analysis and computer security.

ACKNOWLEDGMENTS

This material is based upon work supported by the National Science Foundation under Grant Nos. 1543656 and 1734558.

REFERENCES

- [1] David H. Ackley, Geoffrey E. Hinton, and Terrence J. Sejnowski. 1985. A learning algorithm for boltzmann machines. *Cognitive Science* 9, 1 (1985), 147 – 169. [https://doi.org/10.1016/S0364-0213\(85\)80012-4](https://doi.org/10.1016/S0364-0213(85)80012-4)
- [2] Martin Arjovsky and Léon Bottou. 2017. Towards principled methods for training generative adversarial networks. In *International Conference on Learning Representations*. https://openreview.net/forum?id=Hk4_qw5xe

- [3] Martin Arjovsky, Soumith Chintala, and Léon Bottou. 2017. Wasserstein Generative Adversarial Networks. In *Proceedings of the 34th International Conference on Machine Learning (Proceedings of Machine Learning Research)*, Doina Precup and Yee Whye Teh (Eds.), Vol. 70. PMLR, 214–223. <http://proceedings.mlr.press/v70/arjovsky17a.html>
- [4] Sanjeev Arora, Rong Ge, Yingyu Liang, Tengyu Ma, and Yi Zhang. 2017. Generalization and Equilibrium in Generative Adversarial Nets (GANs). In *Proceedings of the 34th International Conference on Machine Learning (Proceedings of Machine Learning Research)*, Doina Precup and Yee Whye Teh (Eds.), Vol. 70. PMLR, 224–232. <http://proceedings.mlr.press/v70/arora17a.html>
- [5] Sanjeev Arora, Andrej Risteski, and Yi Zhang. 2018. Do GANs learn the distribution? Some Theory and Empirics. In *International Conference on Learning Representations*. <https://openreview.net/forum?id=BJehNfW0->
- [6] Yusuf Aytar, Carl Vondrick, and Antonio Torralba. 2016. SoundNet: Learning Sound Representations from Unlabeled Video. In *Advances in Neural Information Processing Systems 29*, D. D. Lee, M. Sugiyama, U. V. Luxburg, I. Guyon, and R. Garnett (Eds.). Curran Associates, Inc., 892–900. <http://papers.nips.cc/paper/6146-soundnet-learning-sound-representations-from-unlabeled-video.pdf>
- [7] David Balduzzi, Marcus Frean, Lennox Leary, J. P. Lewis, Kurt Wan-Duo Ma, and Brian McWilliams. 2017. The Shattered Gradients Problem: If resnets are the answer, then what is the question?. In *Proceedings of the 34th International Conference on Machine Learning (Proceedings of Machine Learning Research)*, Doina Precup and Yee Whye Teh (Eds.), Vol. 70. PMLR, 342–350. <http://proceedings.mlr.press/v70/balduzzi17b.html>
- [8] Oscar Beijbom. 2012. Domain adaptations for computer vision applications. *arXiv preprint arXiv:1211.4860* (2012).
- [9] Shai Ben-David, John Blitzer, Koby Crammer, Alex Kulesza, Fernando Pereira, and Jennifer Wortman Vaughan. 2010. A theory of learning from different domains. *Machine Learning* 79, 1 (01 May 2010), 151–175. <https://doi.org/10.1007/s10994-009-5152-4>
- [10] Yoshua Bengio and Samy Bengio. 2000. Modeling High-Dimensional Discrete Data with Multi-Layer Neural Networks. In *Advances in Neural Information Processing Systems 12*, S. A. Solla, T. K. Leen, and K. Müller (Eds.). MIT Press, 400–406. <http://papers.nips.cc/paper/1679-modeling-high-dimensional-discrete-data-with-multi-layer-neural-networks.pdf>
- [11] Yoshua Bengio, Eric Laufer, Guillaume Alain, and Jason Yosinski. 2014. Deep Generative Stochastic Networks Trainable by Backprop. In *Proceedings of the 31st International Conference on Machine Learning (Proceedings of Machine Learning Research)*, Eric P. Xing and Tony Jebara (Eds.), Vol. 32. PMLR, 226–234. <http://proceedings.mlr.press/v32/bengio14.html>
- [12] David Berthelot, Tom Schumm, and Luke Metz. 2017. Began: Boundary equilibrium generative adversarial networks. *arXiv preprint arXiv:1703.10717* (2017).
- [13] John Blitzer, Mark Dredze, and Fernando Pereira. 2007. Biographies, bollywood, boom-boxes and blenders: Domain adaptation for sentiment classification. In *Proceedings of the 45th Annual Meeting of the Association of Computational Linguistics*. 440–447.
- [14] Ali Borji. 2018. Pros and Cons of GAN Evaluation Measures. *arXiv preprint arXiv:1802.03446* (2018).
- [15] Konstantinos Bousmalis, Nathan Silberman, David Dohan, Dumitru Erhan, and Dilip Krishnan. 2017. Unsupervised Pixel-Level Domain Adaptation With Generative Adversarial Networks. In *The IEEE Conference on Computer Vision and Pattern Recognition (CVPR)*.
- [16] Konstantinos Bousmalis, George Trigeorgis, Nathan Silberman, Dilip Krishnan, and Dumitru Erhan. 2016. Domain Separation Networks. In *Advances in Neural Information Processing Systems 29*, D. D. Lee, M. Sugiyama, U. V. Luxburg, I. Guyon, and R. Garnett (Eds.). Curran Associates, Inc., 343–351. <http://papers.nips.cc/paper/6254-domain-separation-networks.pdf>
- [17] Rich Caruana. 1997. Multitask Learning. *Machine Learning* 28, 1 (01 Jul 1997), 41–75. <https://doi.org/10.1023/A:1007379606734>
- [18] Minmin Chen, Zhixiang Xu, Kilian Weinberger, and Fei Sha. 2012. Marginalized Denoising Autoencoders for Domain Adaptation. In *Proceedings of the 29th International Conference on Machine Learning (ICML-12) (ICML '12)*, John Langford and Joelle Pineau (Eds.). Omnipress, New York, NY, USA, 767–774.
- [19] Soumith Chintala, Emily Denton, Martin Arjovsky, and Michael Mathieu. 2016. How to train a GAN? Tips and tricks to make GANs work. Retrieved July 26, 2018 from <https://github.com/soumith/ganhacks>
- [20] Junyoung Chung, Kyle Kastner, Laurent Dinh, Kratarth Goel, Aaron C Courville, and Yoshua Bengio. 2015. A Recurrent Latent Variable Model for Sequential Data. In *Advances in Neural Information Processing Systems 28*, C. Cortes, N. D. Lawrence, D. D. Lee, M. Sugiyama, and R. Garnett (Eds.). Curran Associates, Inc., 2980–2988. <http://papers.nips.cc/paper/5653-a-recurrent-latent-variable-model-for-sequential-data.pdf>
- [21] Diane J Cook, Aaron S Crandall, Brian L Thomas, and Narayanan C Krishnan. 2013. CASAS: A Smart Home in a Box. *Computer* 46, 7 (July 2013), 62–69. <https://doi.org/10.1109/MC.2012.328>
- [22] Corinna Cortes and Vladimir Vapnik. 1995. Support-vector networks. *Machine Learning* 20, 3 (01 Sep 1995), 273–297. <https://doi.org/10.1007/BF00994018>

- [23] Hal Daumé III. 2007. Frustratingly Easy Domain Adaptation. In *Proceedings of the 45th Annual Meeting of the Association of Computational Linguistics*. 256–263.
- [24] Hal Daumé III and Daniel Marcu. 2006. Domain Adaptation for Statistical Classifiers. *Journal of Artificial Intelligence Research* 26 (2006), 101–126.
- [25] Gustavo Deco and Wilfried Brauer. 1995. Higher Order Statistical Decorrelation without Information Loss. In *Advances in Neural Information Processing Systems 7*, G. Tesauro, D. S. Touretzky, and T. K. Leen (Eds.). MIT Press, 247–254. <http://papers.nips.cc/paper/901-higher-order-statistical-decorrelation-without-information-loss.pdf>
- [26] J. Deng, W. Dong, R. Socher, L. J. Li, Kai Li, and Li Fei-Fei. 2009. ImageNet: A large-scale hierarchical image database. In *2009 IEEE Conference on Computer Vision and Pattern Recognition*. 248–255. <https://doi.org/10.1109/CVPR.2009.5206848>
- [27] Emily L Denton and Vighnesh Birodkar. 2017. Unsupervised Learning of Disentangled Representations from Video. In *Advances in Neural Information Processing Systems 30*, I. Guyon, U. V. Luxburg, S. Bengio, H. Wallach, R. Fergus, S. Vishwanathan, and R. Garnett (Eds.). Curran Associates, Inc., 4414–4423. <http://papers.nips.cc/paper/7028-unsupervised-learning-of-disentangled-representations-from-video.pdf>
- [28] Emily L Denton, Soumith Chintala, Arthur Szlam, and Rob Fergus. 2015. Deep Generative Image Models using a Laplacian Pyramid of Adversarial Networks. In *Advances in Neural Information Processing Systems 28*, C. Cortes, N. D. Lawrence, D. D. Lee, M. Sugiyama, and R. Garnett (Eds.). Curran Associates, Inc., 1486–1494. <http://papers.nips.cc/paper/5773-deep-generative-image-models-using-a-laplacian-pyramid-of-adversarial-networks.pdf>
- [29] Laurent Dinh, Jascha Sohl-Dickstein, and Samy Bengio. 2016. Density estimation using Real NVP. *arXiv preprint arXiv:1605.08803* (2016).
- [30] Jeff Donahue, Philipp Krähenbühl, and Trevor Darrell. 2017. Adversarial feature learning. In *International Conference on Learning Representations*. <https://openreview.net/forum?id=BJtNZAFgg>
- [31] Mark Dredze, Alex Kulesza, and Koby Crammer. 2010. Multi-domain learning by confidence-weighted parameter combination. *Machine Learning* 79, 1 (01 May 2010), 123–149. <https://doi.org/10.1007/s10994-009-5148-0>
- [32] Vincent Dumoulin, Ishmael Belghazi, Ben Poole, Olivier Mastropietro, Alex Lamb, Martin Arjovsky, and Aaron Courville. 2017. Adversarially learned inference. In *International Conference on Learning Representations*. <https://openreview.net/forum?id=B1ElR4cgg>
- [33] Scott E. Fahlman, Geoffrey E. Hinton, and Terrence J. Sejnowski. 1983. Massively Parallel Architectures for AI: Netl, Thistle, and Boltzmann Machines. In *Proceedings of the Third AAAI Conference on Artificial Intelligence (AAAI'83)*. AAAI Press, 109–113. <http://dl.acm.org/citation.cfm?id=2886844.2886868>
- [34] William Fedus, Mihaela Rosca, Balaji Lakshminarayanan, Andrew M. Dai, Shakir Mohamed, and Ian Goodfellow. 2018. Many Paths to Equilibrium: GANs Do Not Need to Decrease a Divergence At Every Step. In *International Conference on Learning Representations*. <https://openreview.net/forum?id=ByQpn1ZA->
- [35] Chelsea Finn, Paul Christiano, Pieter Abbeel, and Sergey Levine. 2016. A connection between generative adversarial networks, inverse reinforcement learning, and energy-based models. *arXiv preprint arXiv:1611.03852* (2016).
- [36] Brendan J Frey. 1998. *Graphical models for machine learning and digital communication*. MIT Press.
- [37] Yaroslav Ganin and Victor Lempitsky. 2015. Unsupervised Domain Adaptation by Backpropagation. In *Proceedings of the 32nd International Conference on Machine Learning (Proceedings of Machine Learning Research)*, Francis Bach and David Blei (Eds.), Vol. 37. PMLR, 1180–1189. <http://proceedings.mlr.press/v37/ganin15.html>
- [38] Yaroslav Ganin, Evgeniya Ustinova, Hana Ajakan, Pascal Germain, Hugo Larochelle, François Laviolette, Mario Marchand, and Victor Lempitsky. 2016. Domain-Adversarial Training of Neural Networks. *Journal of Machine Learning Research* 17, 59 (2016), 1–35. <http://jmlr.org/papers/v17/15-239.html>
- [39] Leon A. Gatys, Alexander S. Ecker, and Matthias Bethge. 2016. Image Style Transfer Using Convolutional Neural Networks. In *The IEEE Conference on Computer Vision and Pattern Recognition (CVPR)*.
- [40] Jon Gauthier. 2014. Conditional generative adversarial nets for convolutional face generation.
- [41] Mathieu Germain, Karol Gregor, Iain Murray, and Hugo Larochelle. 2015. MADE: Masked Autoencoder for Distribution Estimation. In *Proceedings of the 32nd International Conference on Machine Learning (Proceedings of Machine Learning Research)*, Francis Bach and David Blei (Eds.), Vol. 37. PMLR, 881–889. <http://proceedings.mlr.press/v37/germain15.html>
- [42] Muhammad Ghifary, W. Bastiaan Kleijn, Mengjie Zhang, and David Balduzzi. 2015. Domain Generalization for Object Recognition With Multi-Task Autoencoders. In *The IEEE International Conference on Computer Vision (ICCV)*.
- [43] Muhammad Ghifary, W. Bastiaan Kleijn, Mengjie Zhang, David Balduzzi, and Wen Li. 2016. Deep Reconstruction-Classification Networks for Unsupervised Domain Adaptation. In *Computer Vision – ECCV 2016*, Bastian Leibe, Jiri Matas, Nicu Sebe, and Max Welling (Eds.). Springer International Publishing, Cham, 597–613.
- [44] Ian Goodfellow. 2016. NIPS 2016 tutorial: Generative adversarial networks. *arXiv preprint arXiv:1701.00160* (2016).
- [45] Ian Goodfellow, Jean Pouget-Abadie, Mehdi Mirza, Bing Xu, David Warde-Farley, Sherjil Ozair, Aaron Courville, and Yoshua Bengio. 2014. Generative Adversarial Nets. In *Advances in Neural Information Processing Systems 27*, Z. Ghahramani, M. Welling, C. Cortes, N. D. Lawrence, and K. Q. Weinberger (Eds.). Curran Associates, Inc., 2672–2680.

<http://papers.nips.cc/paper/5423-generative-adversarial-nets.pdf>

- [46] Aditya Grover, Manik Dhar, and Stefano Ermon. 2017. Flow-GAN: Combining maximum likelihood and adversarial learning in generative models. *arXiv preprint arXiv:1705.08868* (2017).
- [47] Liangyan Gui, Kevin Zhang, Yu-Xiong Wang, Xiaodan Liang, José MF Moura, and Manuela M Veloso. 2018. Teaching Robots to Predict Human Motion. (2018). preprint on webpage at <http://www.cs.cmu.edu/~mmv/papers/18iros-GuiEtAl.pdf>.
- [48] Ishaan Gulrajani, Faruk Ahmed, Martin Arjovsky, Vincent Dumoulin, and Aaron C Courville. 2017. Improved Training of Wasserstein GANs. In *Advances in Neural Information Processing Systems 30*, I. Guyon, U. V. Luxburg, S. Bengio, H. Wallach, R. Fergus, S. Vishwanathan, and R. Garnett (Eds.). Curran Associates, Inc., 5767–5777. <http://papers.nips.cc/paper/7159-improved-training-of-wasserstein-gans.pdf>
- [49] Martin Heusel, Hubert Ramsauer, Thomas Unterthiner, Bernhard Nessler, and Sepp Hochreiter. 2017. GANs Trained by a Two Time-Scale Update Rule Converge to a Local Nash Equilibrium. In *Advances in Neural Information Processing Systems 30*, I. Guyon, U. V. Luxburg, S. Bengio, H. Wallach, R. Fergus, S. Vishwanathan, and R. Garnett (Eds.). Curran Associates, Inc., 6626–6637. <http://papers.nips.cc/paper/7240-gans-trained-by-a-two-time-scale-update-rule-converge-to-a-local-nash-equilibrium.pdf>
- [50] Avinash Hindupur. 2018. The GAN Zoo. Retrieved August 16, 2018 from <https://github.com/hindupuravinash/the-gan-zoo>
- [51] Geoffrey E. Hinton. 2012. *A Practical Guide to Training Restricted Boltzmann Machines*. Springer Berlin Heidelberg, Berlin, Heidelberg, 599–619. https://doi.org/10.1007/978-3-642-35289-8_32
- [52] Saifuddin Hitawala. 2018. Comparative Study on Generative Adversarial Networks. *arXiv preprint arXiv:1801.04271* (2018).
- [53] Judy Hoffman, Eric Tzeng, Taesung Park, Jun-Yan Zhu, Phillip Isola, Kate Saenko, Alexei Efros, and Trevor Darrell. 2018. CyCADA: Cycle-Consistent Adversarial Domain Adaptation. In *Proceedings of the 35th International Conference on Machine Learning (Proceedings of Machine Learning Research)*, Jennifer Dy and Andreas Krause (Eds.), Vol. 80. PMLR, 1994–2003. <http://proceedings.mlr.press/v80/hoffman18a.html>
- [54] Yongjun Hong, Uiwon Hwang, Jaeyoon Yoo, and Sungroh Yoon. 2017. How Generative Adversarial Nets and its variants Work: An Overview of GAN. *arXiv preprint arXiv:1711.05914* (2017).
- [55] Ling Huang, Anthony D. Joseph, Blaine Nelson, Benjamin I.P. Rubinstein, and J. D. Tygar. 2011. Adversarial Machine Learning. In *Proceedings of the 4th ACM Workshop on Security and Artificial Intelligence (AISec '11)*. ACM, New York, NY, USA, 43–58. <https://doi.org/10.1145/2046684.2046692>
- [56] Xun Huang, Ming-Yu Liu, Serge Belongie, and Jan Kautz. 2018. Multimodal Unsupervised Image-to-Image Translation. *arXiv preprint arXiv:1804.04732* (2018).
- [57] Phillip Isola, Jun-Yan Zhu, Tinghui Zhou, and Alexei A. Efros. 2017. Image-To-Image Translation With Conditional Adversarial Networks. In *The IEEE Conference on Computer Vision and Pattern Recognition (CVPR)*.
- [58] Jing Jiang. 2008. *Domain adaptation in natural language processing*. Technical Report. University of Illinois at Urbana-Champaign.
- [59] Justin Johnson, Alexandre Alahi, and Li Fei-Fei. 2016. Perceptual Losses for Real-Time Style Transfer and Super-Resolution. In *Computer Vision – ECCV 2016*, Bastian Leibe, Jiri Matas, Nicu Sebe, and Max Welling (Eds.). Springer International Publishing, Cham, 694–711.
- [60] Alexia Jolicoeur-Martineau. 2018. The relativistic discriminator: a key element missing from standard GAN. *arXiv preprint arXiv:1807.00734* (2018).
- [61] Mahesh Joshi, William W. Cohen, Mark Dredze, and Carolyn P. Rosé. 2012. Multi-domain Learning: When Do Domains Matter?. In *Proceedings of the 2012 Joint Conference on Empirical Methods in Natural Language Processing and Computational Natural Language Learning (EMNLP-CoNLL '12)*. Association for Computational Linguistics, Stroudsburg, PA, USA, 1302–1312. <http://dl.acm.org/citation.cfm?id=2390948.2391096>
- [62] Tero Karras, Timo Aila, Samuli Laine, and Jaakko Lehtinen. 2018. Progressive Growing of GANs for Improved Quality, Stability, and Variation. In *International Conference on Learning Representations*. <https://openreview.net/forum?id=Hk99zCeAb>
- [63] Diederik P Kingma and Max Welling. 2013. Auto-encoding variational bayes. *arXiv preprint arXiv:1312.6114* (2013).
- [64] Naveen Kodali, Jacob Abernethy, James Hays, and Zsolt Kira. 2017. On convergence and stability of GANs. *arXiv preprint arXiv:1705.07215* (2017).
- [65] Narayanan C. Krishnan and Diane J. Cook. 2014. Activity recognition on streaming sensor data. *Pervasive and Mobile Computing* 10 (2014), 138 – 154. <https://doi.org/10.1016/j.pmcj.2012.07.003>
- [66] Alex Krizhevsky. 2009. *Learning multiple layers of features from tiny images*. Technical Report.
- [67] David M Kutzik. 2016. Behavioral monitoring to enhance safety and wellness in old age. *Gerontechnology: Research, Practice, and Principles in the Field of Technology and Aging* (2016).

- [68] Hugo Larochelle and Iain Murray. 2011. The Neural Autoregressive Distribution Estimator. In *Proceedings of the Fourteenth International Conference on Artificial Intelligence and Statistics (Proceedings of Machine Learning Research)*, Geoffrey Gordon, David Dunson, and Miroslav Dudík (Eds.), Vol. 15. PMLR, 29–37. <http://proceedings.mlr.press/v15/larochelle11a.html>
- [69] Yann LeCun, Corinna Cortes, and Christopher J.C. Burges. 1998. The MNIST database of handwritten digits. Retrieved August 16, 2018 from <http://yann.lecun.com/exdb/mnist/>
- [70] Y. LeCun, O. Matan, B. Boser, J. S. Denker, D. Henderson, R. E. Howard, W. Hubbard, L. D. Jacket, and H. S. Baird. 1990. Handwritten zip code recognition with multilayer networks. In *[1990] Proceedings. 10th International Conference on Pattern Recognition*, Vol. ii. 35–40 vol.2. <https://doi.org/10.1109/ICPR.1990.119325>
- [71] Christian Ledig, Lucas Theis, Ferenc Huszár, Jose Caballero, Andrew Cunningham, Alejandro Acosta, Andrew Aitken, Alykhan Tejani, Johannes Totz, Zehan Wang, and Wenzhe Shi. 2017. Photo-Realistic Single Image Super-Resolution Using a Generative Adversarial Network. In *The IEEE Conference on Computer Vision and Pattern Recognition (CVPR)*.
- [72] Ming-Yu Liu and Onel Tuzel. 2016. Coupled Generative Adversarial Networks. In *Advances in Neural Information Processing Systems 29*, D. D. Lee, M. Sugiyama, U. V. Luxburg, I. Guyon, and R. Garnett (Eds.). Curran Associates, Inc., 469–477. <http://papers.nips.cc/paper/6544-coupled-generative-adversarial-networks.pdf>
- [73] Shaohui Liu, Yi Wei, Jiwen Lu, and Jie Zhou. 2018. An Improved Evaluation Framework for Generative Adversarial Networks. *arXiv preprint arXiv:1803.07474* (2018).
- [74] Ziwei Liu, Ping Luo, Xiaogang Wang, and Xiaoou Tang. 2015. Deep Learning Face Attributes in the Wild. In *The IEEE International Conference on Computer Vision (ICCV)*.
- [75] Mingsheng Long, Yue Cao, Jianmin Wang, and Michael Jordan. 2015. Learning Transferable Features with Deep Adaptation Networks. In *Proceedings of the 32nd International Conference on Machine Learning (Proceedings of Machine Learning Research)*, Francis Bach and David Blei (Eds.), Vol. 37. PMLR, 97–105. <http://proceedings.mlr.press/v37/long15.html>
- [76] William Lotter, Gabriel Kreiman, and David Cox. 2015. Unsupervised learning of visual structure using predictive generative networks. *arXiv preprint arXiv:1511.06380* (2015).
- [77] Mario Lucic, Karol Kurach, Marcin Michalski, Sylvain Gelly, and Olivier Bousquet. 2017. Are GANs Created Equal? A Large-Scale Study. *arXiv preprint arXiv:1711.10337* (2017).
- [78] Alireza Makhzani, Jonathon Shlens, Navdeep Jaitly, Ian Goodfellow, and Brendan Frey. 2015. Adversarial autoencoders. *arXiv preprint arXiv:1511.05644* (2015).
- [79] P Manisha and Sujit Gujar. 2018. Generative Adversarial Networks (GANs): What it can generate and What it cannot? *arXiv preprint arXiv:1804.00140* (2018).
- [80] Yishay Mansour, Mehryar Mohri, and Afshin Rostamizadeh. 2009. Domain Adaptation with Multiple Sources. In *Advances in Neural Information Processing Systems 21*, D. Koller, D. Schuurmans, Y. Bengio, and L. Bottou (Eds.). Curran Associates, Inc., 1041–1048. <http://papers.nips.cc/paper/3550-domain-adaptation-with-multiple-sources.pdf>
- [81] Anna Margolis. 2011. A Literature Review of Domain Adaptation with Unlabeled Data.
- [82] Luke Metz, Ben Poole, David Pfau, and Jascha Sohl-Dickstein. 2017. Unrolled generative adversarial networks. In *International Conference on Learning Representations*. <https://openreview.net/forum?id=BydrOIcIe>
- [83] Mehdi Mirza and Simon Osindero. 2014. Conditional generative adversarial nets. *arXiv preprint arXiv:1411.1784* (2014).
- [84] Takeru Miyato, Toshiki Kataoka, Masanori Koyama, and Yuichi Yoshida. 2018. Spectral Normalization for Generative Adversarial Networks. In *International Conference on Learning Representations*. <https://openreview.net/forum?id=B1QRgzIT->
- [85] Takeru Miyato and Masanori Koyama. 2018. cGANs with Projection Discriminator. In *International Conference on Learning Representations*. <https://openreview.net/forum?id=ByS1VpgRZ>
- [86] Boris Moiseev, Artem Konev, Alexander Chigorin, and Anton Konushin. 2013. Evaluation of Traffic Sign Recognition Methods Trained on Synthetically Generated Data. In *Advanced Concepts for Intelligent Vision Systems*, Jacques Blanc-Talon, Andrzej Kasinski, Wilfried Philips, Dan Popescu, and Paul Scheunders (Eds.). Springer International Publishing, Cham, 576–583.
- [87] Krikamol Muandet, David Balduzzi, and Bernhard Schölkopf. 2013. Domain Generalization via Invariant Feature Representation. In *Proceedings of the 30th International Conference on Machine Learning (Proceedings of Machine Learning Research)*, Sanjoy Dasgupta and David McAllester (Eds.), Vol. 28. PMLR, 10–18. <http://proceedings.mlr.press/v28/muandet13.html>
- [88] Yuval Netzer, Tao Wang, Adam Coates, Alessandro Bissacco, Bo Wu, and Andrew Y Ng. 2011. Reading digits in natural images with unsupervised feature learning. In *NIPS workshop on deep learning and unsupervised feature learning*, Vol. 2011. 5.
- [89] Andrew Y Ng and Stuart J Russell. 2000. Algorithms for Inverse Reinforcement Learning. In *Proceedings of the Seventeenth International Conference on Machine Learning*. Morgan Kaufmann Publishers Inc., 663–670.

- [90] Sebastian Nowozin, Botond Cseke, and Ryota Tomioka. 2016. f-GAN: Training Generative Neural Samplers using Variational Divergence Minimization. In *Advances in Neural Information Processing Systems 29*, D. D. Lee, M. Sugiyama, U. V. Luxburg, I. Guyon, and R. Garnett (Eds.). Curran Associates, Inc., 271–279. <http://papers.nips.cc/paper/6066-f-gan-training-generative-neural-samplers-using-variational-divergence-minimization.pdf>
- [91] Augustus Odena, Jacob Buckman, Catherine Olsson, Tom Brown, Christopher Olah, Colin Raffel, and Ian Goodfellow. 2018. Is Generator Conditioning Causally Related to GAN Performance?. In *Proceedings of the 35th International Conference on Machine Learning (Proceedings of Machine Learning Research)*, Jennifer Dy and Andreas Krause (Eds.), Vol. 80. PMLR, 3846–3855. <http://proceedings.mlr.press/v80/odena18a.html>
- [92] Augustus Odena, Christopher Olah, and Jonathon Shlens. 2017. Conditional Image Synthesis with Auxiliary Classifier GANs. In *Proceedings of the 34th International Conference on Machine Learning (Proceedings of Machine Learning Research)*, Doina Precup and Yee Whye Teh (Eds.), Vol. 70. PMLR, 2642–2651. <http://proceedings.mlr.press/v70/odena17a.html>
- [93] Frans A Oliehoek, Rahul Savani, Jose Gallego, Elise van der Pol, and Roderich Groß. 2018. Beyond Local Nash Equilibria for Adversarial Networks. *arXiv preprint arXiv:1806.07268* (2018).
- [94] Aaron Van Oord, Nal Kalchbrenner, and Koray Kavukcuoglu. 2016. Pixel Recurrent Neural Networks. In *Proceedings of The 33rd International Conference on Machine Learning (Proceedings of Machine Learning Research)*, Maria Florina Balcan and Kilian Q. Weinberger (Eds.), Vol. 48. PMLR, New York, New York, USA, 1747–1756. <http://proceedings.mlr.press/v48/oord16.html>
- [95] E. Osuna, R. Freund, and F. Girosi. 1997. An improved training algorithm for support vector machines. In *Neural Networks for Signal Processing VII. Proceedings of the 1997 IEEE Signal Processing Society Workshop*. 276–285. <https://doi.org/10.1109/NNSP.1997.622408>
- [96] Sinno Jialin Pan and Qiang Yang. 2010. A Survey on Transfer Learning. *IEEE Transactions on Knowledge and Data Engineering* 22, 10 (Oct 2010), 1345–1359. <https://doi.org/10.1109/TKDE.2009.191>
- [97] V. M. Patel, R. Gopalan, R. Li, and R. Chellappa. 2015. Visual Domain Adaptation: A survey of recent advances. *IEEE Signal Processing Magazine* 32, 3 (May 2015), 53–69. <https://doi.org/10.1109/MSP.2014.2347059>
- [98] David Pfau and Oriol Vinyals. 2016. Connecting generative adversarial networks and actor-critic methods. *arXiv preprint arXiv:1610.01945* (2016).
- [99] L. Pinto, J. Davidson, and A. Gupta. 2017. Supervision via competition: Robot adversaries for learning tasks. In *2017 IEEE International Conference on Robotics and Automation (ICRA)*. 1601–1608. <https://doi.org/10.1109/ICRA.2017.7989190>
- [100] Sanjay Purushotham, Wilka Carvalho, Tanachat Nilanon, and Yan Liu. 2017. Variational adversarial deep domain adaptation for health care time series analysis. In *International Conference on Learning Representations*. <https://openreview.net/forum?id=rk9eAFcxg>
- [101] Alec Radford, Luke Metz, and Soumith Chintala. 2015. Unsupervised representation learning with deep convolutional generative adversarial networks. *arXiv preprint arXiv:1511.06434* (2015).
- [102] Danilo Jimenez Rezende, Shakir Mohamed, and Daan Wierstra. 2014. Stochastic Backpropagation and Approximate Inference in Deep Generative Models. In *Proceedings of the 31st International Conference on Machine Learning (Proceedings of Machine Learning Research)*, Eric P. Xing and Tony Jebara (Eds.), Vol. 32. PMLR, 1278–1286. <http://proceedings.mlr.press/v32/rezende14.html>
- [103] Oren Rippel and Lubomir Bourdev. 2017. Real-Time Adaptive Image Compression. In *Proceedings of the 34th International Conference on Machine Learning (Proceedings of Machine Learning Research)*, Doina Precup and Yee Whye Teh (Eds.), Vol. 70. PMLR, 2922–2930. <http://proceedings.mlr.press/v70/rippel17a.html>
- [104] Oren Rippel, Lubomir Bourdev, Carissa Lew, and Sanjay Nair. 2018. Using generative adversarial networks in compression. US Patent App. 15/844,449.
- [105] Stéphane Ross, Geoffrey Gordon, and Drew Bagnell. 2011. A Reduction of Imitation Learning and Structured Prediction to No-Regret Online Learning. In *Proceedings of the Fourteenth International Conference on Artificial Intelligence and Statistics (Proceedings of Machine Learning Research)*, Geoffrey Gordon, David Dunson, and Miroslav Dudík (Eds.), Vol. 15. PMLR, 627–635. <http://proceedings.mlr.press/v15/ross11a.html>
- [106] Artem Rozantsev, Mathieu Salzmann, and Pascal Fua. 2018. Beyond Sharing Weights for Deep Domain Adaptation. *IEEE Transactions on Pattern Analysis and Machine Intelligence* (2018), 1–1. <https://doi.org/10.1109/TPAMI.2018.2814042>
- [107] Olga Russakovsky, Jia Deng, Hao Su, Jonathan Krause, Sanjeev Satheesh, Sean Ma, Zhiheng Huang, Andrej Karpathy, Aditya Khosla, Michael Bernstein, Alexander C. Berg, and Li Fei-Fei. 2015. ImageNet Large Scale Visual Recognition Challenge. *International Journal of Computer Vision (IJCV)* 115, 3 (2015), 211–252. <https://doi.org/10.1007/s11263-015-0816-y>
- [108] Kate Saenko, Brian Kulis, Mario Fritz, and Trevor Darrell. 2010. Adapting Visual Category Models to New Domains. In *Computer Vision – ECCV 2010*, Kostas Daniilidis, Petros Maragos, and Nikos Paragios (Eds.). Springer Berlin Heidelberg, Berlin, Heidelberg, 213–226.

- [109] Kuniaki Saito, Yoshitaka Ushiku, and Tatsuya Harada. 2017. Asymmetric Tri-training for Unsupervised Domain Adaptation. In *Proceedings of the 34th International Conference on Machine Learning (Proceedings of Machine Learning Research)*, Doina Precup and Yee Whye Teh (Eds.), Vol. 70. PMLR, 2988–2997. <http://proceedings.mlr.press/v70/saito17a.html>
- [110] Tim Salimans, Ian Goodfellow, Wojciech Zaremba, Vicki Cheung, Alec Radford, Xi Chen, and Xi Chen. 2016. Improved Techniques for Training GANs. In *Advances in Neural Information Processing Systems 29*, D. D. Lee, M. Sugiyama, U. V. Luxburg, I. Guyon, and R. Garnett (Eds.). Curran Associates, Inc., 2234–2242. <http://papers.nips.cc/paper/6125-improved-techniques-for-training-gans.pdf>
- [111] Shibani Santurkar, Ludwig Schmidt, and Aleksander Madry. 2018. A Classification-Based Study of Covariate Shift in GAN Distributions. In *Proceedings of the 35th International Conference on Machine Learning (Proceedings of Machine Learning Research)*, Jennifer Dy and Andreas Krause (Eds.), Vol. 80. PMLR, 4487–4496. <http://proceedings.mlr.press/v80/santurkar18a.html>
- [112] Ashish Shrivastava, Tomas Pfister, Oncel Tuzel, Joshua Susskind, Wenda Wang, and Russell Webb. 2017. Learning From Simulated and Unsupervised Images Through Adversarial Training. In *The IEEE Conference on Computer Vision and Pattern Recognition (CVPR)*.
- [113] J. Stallkamp, M. Schlipsing, J. Salmen, and C. Igel. 2011. The German Traffic Sign Recognition Benchmark: A multi-class classification competition. In *The 2011 International Joint Conference on Neural Networks*. 1453–1460. <https://doi.org/10.1109/IJCNN.2011.6033395>
- [114] Baochen Sun, Jiashi Feng, and Kate Saenko. 2016. Return of Frustratingly Easy Domain Adaptation. In *AAAI Conference on Artificial Intelligence*. <https://www.aaai.org/ocs/index.php/AAAI/AAAI16/paper/view/12443>
- [115] Baochen Sun and Kate Saenko. 2016. Deep CORAL: Correlation Alignment for Deep Domain Adaptation. In *Computer Vision – ECCV 2016 Workshops*, Gang Hua and Hervé Jégou (Eds.). Springer International Publishing, Cham, 443–450.
- [116] Christian Szegedy, Vincent Vanhoucke, Sergey Ioffe, Jon Shlens, and Zbigniew Wojna. 2016. Rethinking the Inception Architecture for Computer Vision. In *The IEEE Conference on Computer Vision and Pattern Recognition (CVPR)*.
- [117] Lucas Theis, Aäron van den Oord, and Matthias Bethge. 2016. A note on the evaluation of generative models. In *International Conference on Learning Representations*. <https://arxiv.org/abs/1511.01844>
- [118] Eric Tzeng, Judy Hoffman, Trevor Darrell, and Kate Saenko. 2015. Simultaneous Deep Transfer Across Domains and Tasks. In *The IEEE International Conference on Computer Vision (ICCV)*.
- [119] Eric Tzeng, Judy Hoffman, Kate Saenko, and Trevor Darrell. 2017. Adversarial Discriminative Domain Adaptation. In *The IEEE Conference on Computer Vision and Pattern Recognition (CVPR)*.
- [120] Carl Vondrick, Hamed Pirsiavash, and Antonio Torralba. 2016. Generating Videos with Scene Dynamics. In *Advances in Neural Information Processing Systems 29*, D. D. Lee, M. Sugiyama, U. V. Luxburg, I. Guyon, and R. Garnett (Eds.). Curran Associates, Inc., 613–621. <http://papers.nips.cc/paper/6194-generating-videos-with-scene-dynamics.pdf>
- [121] Xiaolong Wang, Abhinav Shrivastava, and Abhinav Gupta. 2017. A-Fast-RCNN: Hard Positive Generation via Adversary for Object Detection. In *The IEEE Conference on Computer Vision and Pattern Recognition (CVPR)*.
- [122] Karl Weiss, Taghi M. Khoshgoftaar, and DingDing Wang. 2016. A survey of transfer learning. *Journal of Big Data* 3, 1 (28 May 2016), 9. <https://doi.org/10.1186/s40537-016-0043-6>
- [123] Yuhuai Wu, Yuri Burda, Ruslan Salakhutdinov, and Roger Grosse. 2017. On the quantitative analysis of decoder-based generative models. In *International Conference on Learning Representations*. <https://openreview.net/forum?id=B1M8JF9xx>
- [124] Yongxin Yang and Timothy M Hospedales. 2015. A unified perspective on multi-domain and multi-task learning. In *International Conference on Learning Representations*. <https://arxiv.org/abs/1412.7489>
- [125] Fisher Yu, Ari Seff, Yinda Zhang, Shuran Song, Thomas Funkhouser, and Jianxiong Xiao. 2015. Lsun: Construction of a large-scale image dataset using deep learning with humans in the loop. *arXiv preprint arXiv:1506.03365* (2015).
- [126] Han Zhang, Ian Goodfellow, Dimitris Metaxas, and Augustus Odena. 2018. Self-Attention Generative Adversarial Networks. *arXiv preprint arXiv:1805.08318* (2018).
- [127] Junbo Zhao, Michael Mathieu, and Yann LeCun. 2017. Energy-based generative adversarial network. In *International Conference on Learning Representations*. <https://openreview.net/forum?id=ryh9pmcee>
- [128] Mingmin Zhao, Shichao Yue, Dina Katabi, Tommi S. Jaakkola, and Matt T. Bianchi. 2017. Learning Sleep Stages from Radio Signals: A Conditional Adversarial Architecture. In *Proceedings of the 34th International Conference on Machine Learning (Proceedings of Machine Learning Research)*, Doina Precup and Yee Whye Teh (Eds.), Vol. 70. PMLR, 4100–4109. <http://proceedings.mlr.press/v70/zhao17d.html>
- [129] Jun-Yan Zhu, Taesung Park, Phillip Isola, and Alexei A. Efros. 2017. Unpaired Image-To-Image Translation Using Cycle-Consistent Adversarial Networks. In *The IEEE International Conference on Computer Vision (ICCV)*.